Final Report SM-46220-F

INORGANIC SEPARATOR FOR HIGH TEMPERATURE SILVER-ZINC BATTERY

National Aeronautics and Space Administration
Contract NAS 3-6007

September 1965

N66 10655

MISSILE & SPACE SYSTEMS DIVISION
ASTROPOWER LABORATORY
Douglas Aircraft Company, Inc.
Newport Beach, California

FOREWORD

This report was prepared under Project Work Order Number 177067-01 and covers the period 7/27/64 through 7/29/65. The research, development and testing effort discussed in this report was sponsored by Lewis Research Center, National Aeronautics & Space Administration, Cleveland, Ohio.

TABLE OF CONTENTS

TABLE OF CONTENTS (Continued)

LIST OF ILLUSTRATIONS

LIST OF ILLUSTRATIONS (Continued)

LIST OF ILLUSTRATIONS (Continued)

LIST OF TABLES

1.0 INTRODUCTION AND SUMMARY

1.1 Douglas Battery Research and Development

In 1962 Astropower Laboratory, Missile and Space System Division, Douglas Aircraft Company, undertook an advanced research and development program devoted to silver-zinc, silver-cadmium, and nickel-cadmium batteries. Particular emphasis was placed on the silver-zinc system as it offers the greatest potential for space application due to its high energy density per unit weight and volume.(1) Utilization of silver-zinc batteries in space, military and commercial applications has been limited, however, because of its short cycle life, inability to withstand deep discharge and temperature sensitivity which limits its use in normal ambient temperatures.(2) These limitations are mainly related to the organic separators used and it is widely recognized that conventional separators such as sausage casing and cellophane are the weak point of alkaline cell design which has prevented advanced development and widescale application of silver-zinc batteries.(3)

Douglas silver-zinc battery programs(4, 5, 6) are devoted to the research and development of inorganic separators and novel electrode configurations. The objectives of these programs include:

1. Long cycle life at normal ambient temperature
2. Long cycle life at 100°C
3. Deep discharge capability
4. High temperature operation
5. Long wet stand capability and good charge retention

1.1.1 Cycle Life of Silver-Zinc Cells at 25° and 100°C

This work resulted in the development of silver-zinc test cells capable of more than 1800 charge-discharge cycles at room temperature and 1700 cycles at 100°C at 20 ma/cm^2 and 20% depth of discharge. In comparison, conventional silver-zinc cells which utilize cellophane, sausage casing and other organic separators are capable of limited cycle life at normal ambient temperature, usually failing after 8 to 10 cycles although some investigators have reported experimental silver-zinc cells capable of 100-200 cycles.(7) These cells apparently are constructed with many layers of organic separators or use specially treated cellophane and other similar materials.

Based on the results obtained thus far with cells constructed with inorganic separators, it is reasonable to project ultimate cycle life of 5000 cycles or more at temperatures ranging from ambient to 100°C.

1.1.2 Deep Discharge Capability

Limited tests indicate that these cells are capable of long cycle life at 50% or greater depth of discharge. Test cells have been run for 528 cycles at 50% depth of discharge at 25°C without deterioration and these tests are continuing. Other tests at 100% depth of discharge have exceeded 50 cycles at 25°C and are still in process.

1.1.3 High Temperature Operation

Preliminary cycle tests at 125° and 150°C indicate that these cells can be operated satisfactorily at temperatures as high as 150°C. As these tests were run using open or unsealed cells, cycle life was limited due to the difficulty of maintaining electrolyte in the test cells at temperatures above the boiling point of the electrolyte. However, more than 50 cycles were obtained at 125°C and 25 cycles at 150°C. Considerably improved cycle life performance can be anticipated using sealed cells where maintenance of the electrolyte is not a problem. It is also indicated by the work done in this program that additional research and development related to zinc electrodes may be necessary, particularly for operation at high temperature.

1.1.4 Environmental Testing of Silver-Zinc Multiplate Batteries

Multiplate batteries having the same overall physical dimensions as conventional batteries were subjected to a typical vibration test schedule used for qualification of space batteries. This test specification is given in Appendix A. Complete battery assemblies as well as battery assemblies containing only the inorganic separators both dry and fully saturated with KOH, passed these tests in all orientations. These results reinforce the anticipation that silver-zinc batteries fabricated using Douglas inorganic separators and electrode configurations will be rugged and fully capable of meeting space battery qualification tests.

1.1.5 Thermal Sterilization of Silver-Zinc Cells

Although not a direct objective of these programs, limited thermal sterilization tests were made on silver-zinc test cells utilizing inorganic separators. It was found that these cells successfully survived heat sterilization for three 33-hour cycles at 145°C in accordance with JPL Specification XS0-30275-TSTA in both the activated and dry state. Figure 1 shows typical performance for silver-zinc test cells which have been dry sterilized according to this procedure.

1.2 NASA Lewis Program (NAS 3-6007)

A proposal was submitted to NASA-Lewis outlining a program devoted to the validation of these findings(8). This proposal resulted in sponsorship of a program "Inorganic Separator for a High Temperature Silver-Zinc Battery" under Contract NAS 3-6007. Work on this contract was started on 29 June 1964 and was concluded 29 July 1965. The principle objectives of the program were:

1. Validation of silver-zinc test cell cycle test results at 25° and 100°C and operating characteristics in the temperature range 25° - 150°C previously obtained under Douglas sponsored programs.

2. Increased emphasis on the quality control aspects of separator and electrode preparation in order to insure a high level of reproducibility of results.

3. Evaluation of silver-zinc test cells fabricated from improved components at 25° and 100°C at 25% and 50% depth of discharge on 1/2 hour discharge - 1/2 hour charge cycle test. 1500 cycles was established as the goal for cycle life at 100°C.

4. Performance characteristics of silver-zinc test cells at 25°, 50°, 100°, 125° and 150°C at 25% and 50% depth of discharge.

These objectives as well as the others specified in the NAS 3-6007 work statement, have been satisfactorily achieved.

Silver-zinc test cells have been cycled for more than 2700 times at 25°C and 2280 cycles at 100°C at approximately 20 ma/cm^2 current density and 20% depth of discharge.

Inorganic separator processing and fabrication techniques have been improved, resulting in the production of separators of good quality, uniformity, and reproducibility.

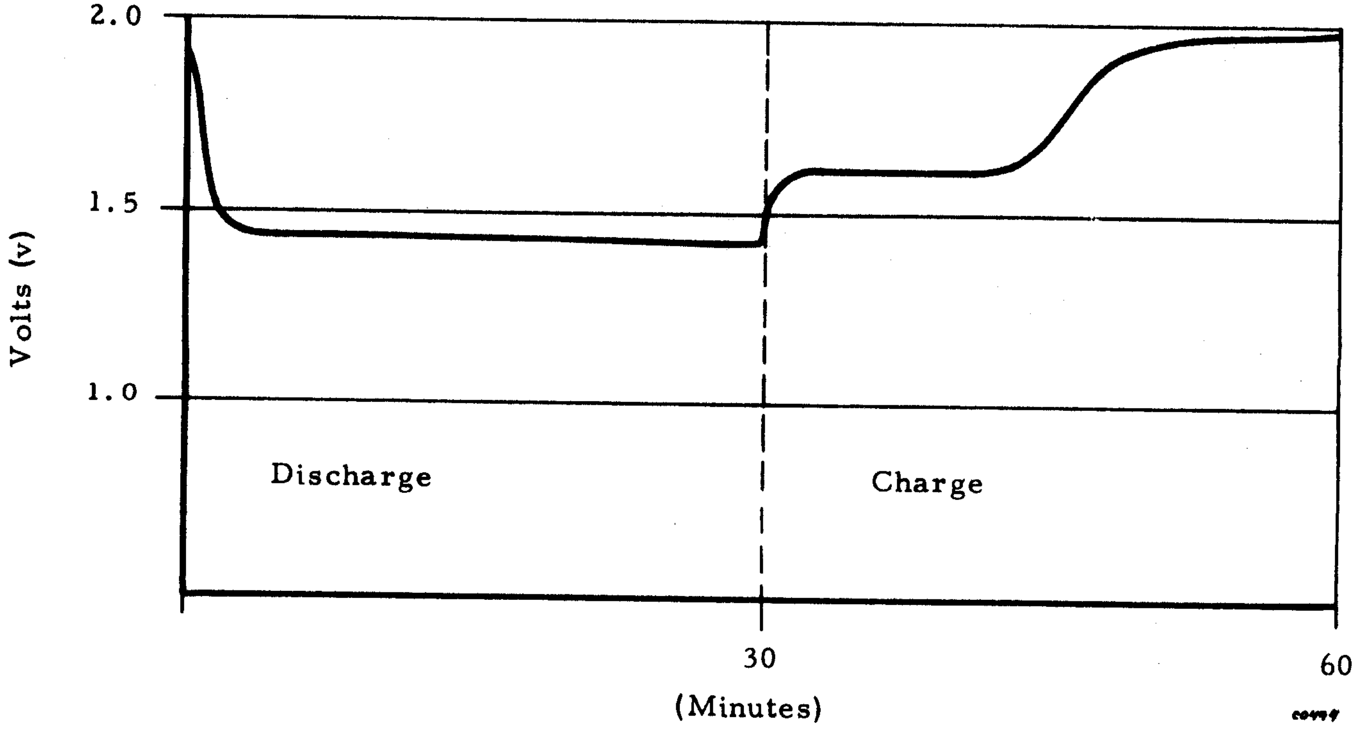

Figure 1. Discharge-Charge Curve Silver-Zinc Test Cell 187354
Following Heat Sterilization per JPL Spec. XSO-30275-TST-A

Test cells have been characterized at 25°, 50°, and 100°C and limited evaluations have been made at 125° and 150°C. Satisfactory performance has also been obtained at 25% and 50% depth of discharge.

Limited tests related to electode gassing characteristics were run at 25° and 100°C in order to compare Douglas electrodes with electrodes removed from a typical, commercial 5 AH high rate silver-zinc cell. These tests indicated superior gassing behavior of Douglas electrodes at both temperatures.

More work, however, will be performed in all of these areas under Contract NAS 3-7639 with particular emphasis on improvement of zinc electrodes, inorganic separator processing and design.

2.0 TECHNICAL DISCUSSION

Astropower Laboratory, Missile & Space Systems Division, Douglas Aircraft Company has been investigating high energy density battery systems since 1962 with the objective of improving cycle life, developing capability for operation at elevated temperatures, deep discharge capability and improving operating characteristics and energy density per unit weight and volume(4, 5, 6). This work has resulted in the development of inorganic separators and electrode configurations which show much promise for space battery application, especially in the silver-zinc and silver-cadmium systems.

2.1 Inorganic Separators

The separators used in this program were fabricated from a proprietary formulation previously developed and identified as Type 5-036-011.

2.1.1 Inorganic Battery Separator Fabrication

Test cell separators were prepared by dry ball milling the No. 5-036-011 formulation for 15 hours, granulating the milled material along with a small amount of Carbowax 4000 to a (-) 32(+)80 mesh screen separation and compacting at 15 tons total load in a 2-inch diameter steel die. After compaction, the separators were placed on smooth refractory surfaces and sintered at about 1100°C in an electric muffle furnace or a gas-air high temperature furnace. Figure 2 is a photograph of the gas-air furnace used for sintering. Figure 3 shows the hydraulic press and pressing dies used and Figure 4 is a photograph of typical 2-inch diameter inorganic battery separators used in the cells tested in this program.

2.1.2 Inspection and Testing of Inorganic Separators

In order to provide separators of high quality having a high level of uniformity for evaluation in test cells, appropriate quality control tests and inspection procedures were established. These tests and procedures included:

A. Moisture Control of Compacting Materials

The moisture control of each lot of compacting material was determined by measuring the weight loss after drying to constant weight at 110°C. The percentage of water present in the compacting mix was determined in accordance with ASTM Specification C20-46.

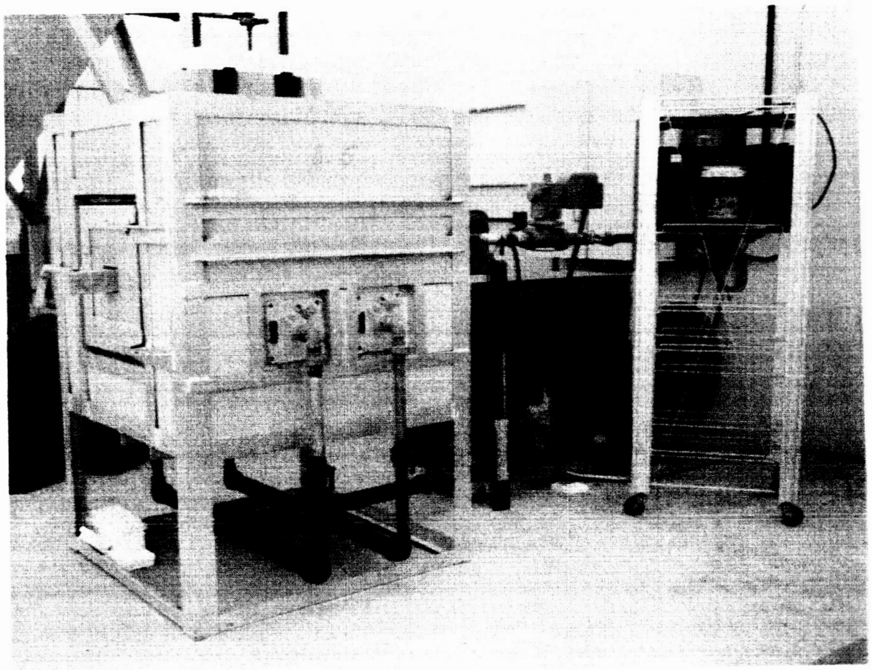

C1064

Figure 2. High Temperature Sintering Furnace

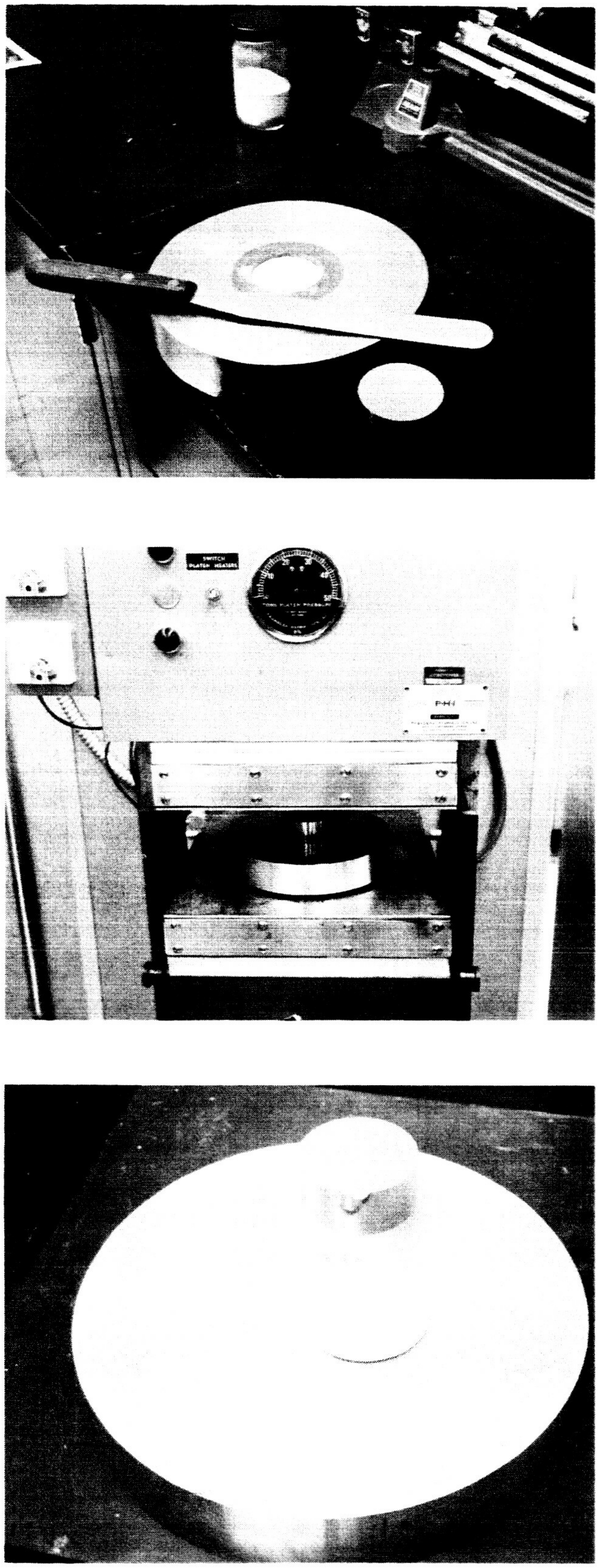

c1066

Figure 3. Mold and Hydraulic Press Used for Compacting Inorganic Battery Separators

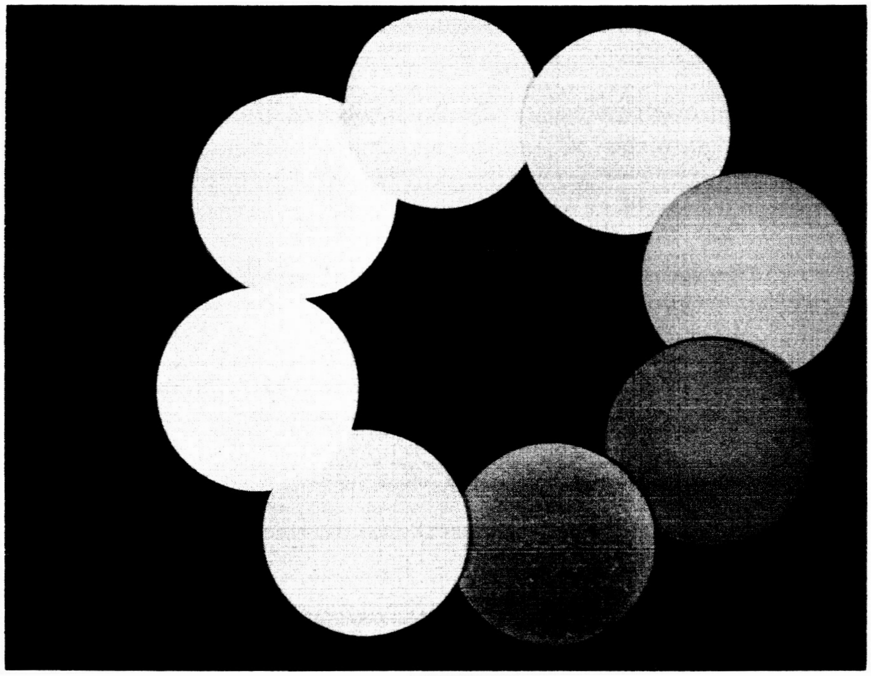

C1065

Figure 4. Two-inch Diameter Inorganic Battery Separators

B. Porosity of Sintered Inorganic Separators

The porosity of sintered inorganic separators was determined by measuring the percent water absorption in accordance with ASTM specification C20-46.

C. Transverse Strength of Inorganic Separators

The transverse strength of each lot of inorganic separators was determined by testing approximately 10% of each lot selected at random. Test specimens 0.500 ± 0.001 inches wide were cut from the 2-inch diameter separators using a diamond saw. These specimens were then broken on the transverse strength testing machine shown in Figure 5. The modulus of Rupture was calculated according to the equation,

$$M = \frac{3pl}{2b\,d^2} \quad \text{where,} \qquad (1)$$

M = modulus of rupture (psi)
P = breaking load (pounds)
l = span (inches)
b = breadth (inches)
d = thickness (inches)

D. Permeability of Inorganic Separators

As the permeability of the separators used has a critical effect on the performance of a battery, the permeability of the inorganic separators used in this program was evaluated using a nitrogen porosimeter. The apparatus shown in Figure 6 determines permeability by measuring the pressure drop through the test specimen.

E. Dimensional Inspection of Inorganic Separators

The separators used in this program were subjected to 100% dimensional inspection by measuring the thickness of each of the discs at the center point and at 4 positions at 90° intervals near the edge.

F. Visual Inspection of Inorganic Separators

The inorganic separators used in this program were examined visually as well as with a 20-power binocular microscope and

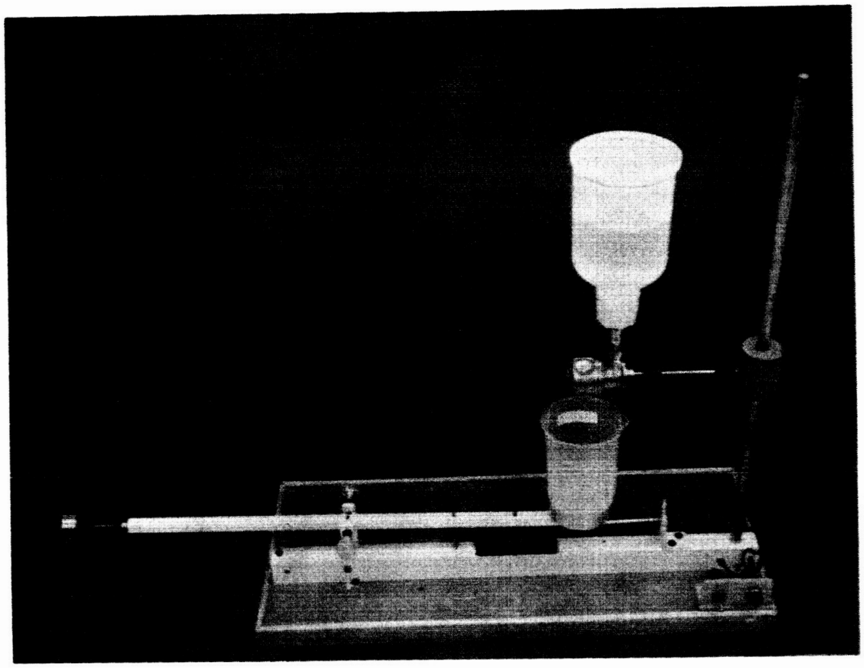

C1136

Figure 5. Apparatus for Measuring Transverse Strength of Inorganic Battery Separators

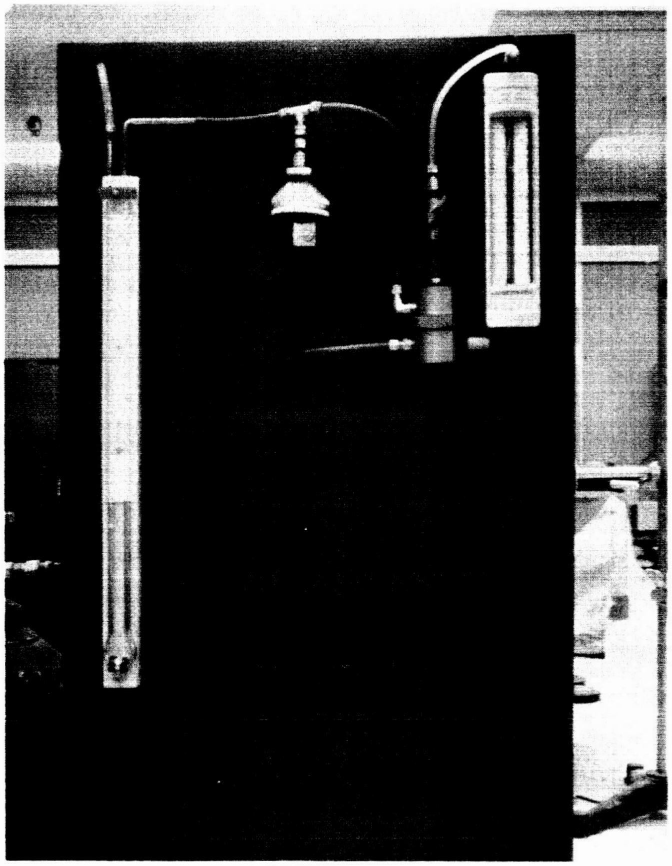

C1137

Figure 6. Gas Porosimeter for Measuring Permeability of Inorganic Battery Separators

with transmitted light. All visual inspections were performed on a 100% basis in order to eliminate defects such as pits, spots, cracks, chips, contamination and surface irregularities.

2.1.3 Effect of Processing Procedures on Inorganic Separator Characteristics

One of the major advantages of the inorganic separator approach to the development of improved high-energy density batteries, is that the physical characteristics of the separator system, such as strength, porosity and permeability can be readily varied by changing processing procedures. This unique capability makes it possible to prepare separators having characteristics exactly tailored to the application and permits wide lattitude in cell design.

This capability is illustrated by the results obtained when the effects of compacting pressure and sintering temperatures on transverse strength, porosity and permeability were investigated. Figure 7 shows the effect of sintering temperature and compacting pressure on the transverse strength of No. 5-036-011 inorganic separators. As shown in this figure, and in Table I, increased compacting pressure in the range of 15 to 50 tons, results in increased transverse strength at the four sintering temperatures investigated (925°, 985°, 1040°, and 1095°C).

As anticipated for a sintered inorganic structure, high separator strength is related to high compacting pressure and high sintering temperature. Separator strength ranged from about 3500 psi to nearly 9000 psi with the bulk of the data falling mid-range for both compacting pressure and sintering temperature.

The effects of the compacting pressure and sintering temperature used in fabricating inorganic battery separators of Type No. 5-036-011 formulation on porosity and permeability were also investigated. It was found, as shown in Figure 8, that both porosity and permeability decreased as the compacting pressure was increased from 15 tons to 50 tons. Both porosity and permeability also decreased as the sintering temperature was increased from 985° to 1095°C. As anticipated for a sintered inorganic compact, increases in compacting pressure and sintering temperature have

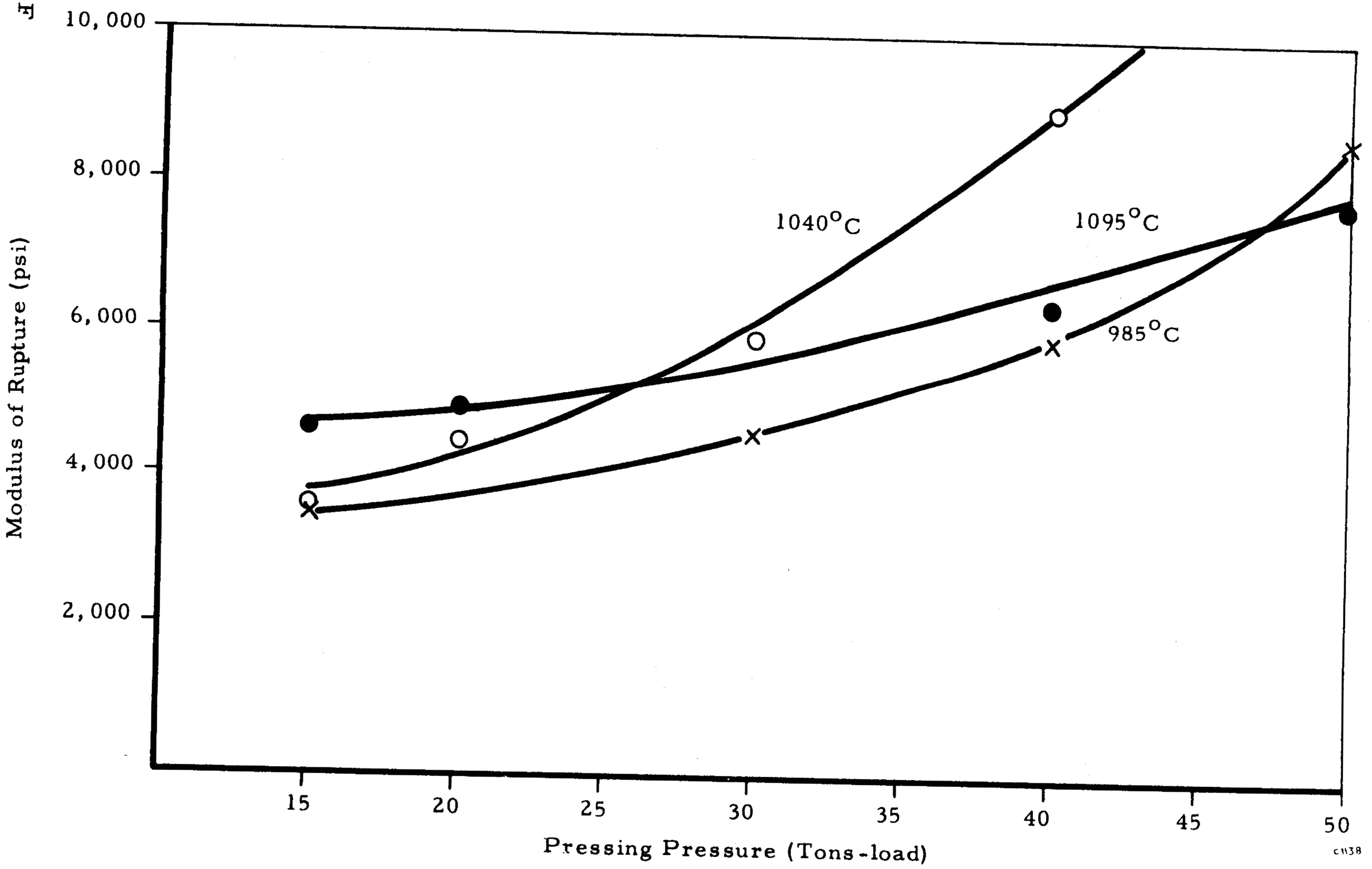

Figure 7. Effect of Sintering Temperature and Compacting Pressure on Transverse Strength of No. 5-036-011 Battery Separators

TABLE I

EFFECT OF COMPACTING PRESSURE AND SINTERING TEMPERATURE ON STRENGTH OF INORGANIC SEPARATORS

Pressing Presure (tons)		Modulus of Rupture (psi)			
	Sintering temperature	925°C	985°C	1040°C	1095°C
15		*	3455	3680	4650
20		*	- - -	4566	4910
30		*	4600	5950	5600
40		*	5983	8903	6700
50		*	8670	- -	8000

* Weak-not measured

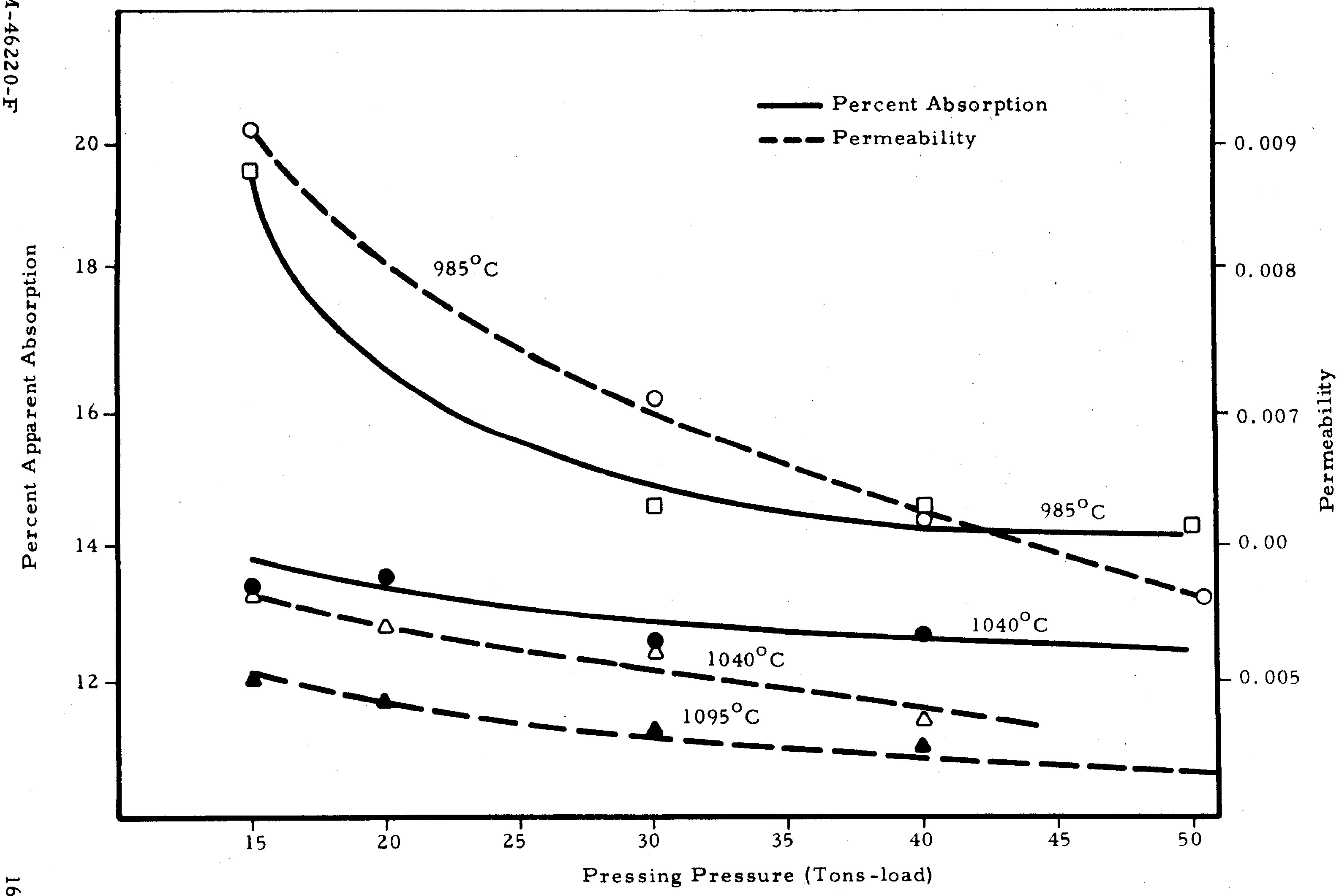

Figure 8. Effect of Sintering Temperature and Pressing Pressure on Apparent Absorption and Gas Permeability of 5-036-011 Battery Separators

a substantially greater effect on porosity and permeability in the lower ranges. The effect of increasing the pressing pressure on these characteristics is quite small in the 11.5-13.5% absorption range. This indicates that the control of separator porosity and permeability results from control of the sintering time-temperature schedule and that only nominal control of pressing pressure is necessary in order to assure a high level of separator uniformity.

2.1.4 Quality Control and Inspection

The quality control tests and final inspection of inorganic separators used in the cells tested in this program were performed as previously described in Section 2.1.2. Briefly, material control consisted of careful weighing, mixing and milling of the formulation, granulation in accordance with standardized procedures and control of the moisture content of the granulated compacting batch to ± 1%. As contamination with foreign material must be carefully avoided to eliminate spots, pits and inclusion, high standards of cleanliness were observed throughout the material preparation and handling process.

Separator compacting pressure was manually controlled by means of the hydraulic gauge on the press to an estimated accuracy of ± 500 pounds. As discussed previously, small changes in compacting pressure have little effect on separator strength, absorption and permeability in the range used and this degree of control is adaquate for uniform results.

In order to compensate for any lack of flatness and parallelity of the press plates or compacting tooling, the separators were compacted twice - the second pressing taking place after the die was rotated 90° from the first pressing position.

Separator sintering was controlled by using a time-temperature heating and cooling schedule which had previously been established experimentally. Sintering temperature was measured with a Wheelco indicator-controller and a chromel-alumel thermocouple in the case of the electrical muffle furnaces and L&N volt-potentiometer was used as a standard for accuracy verification. Sintering temperatures in the gas-air furnace were measured with a platinum-platinum, 13% rhodium thermocouple and a L&N volt-potentiometer. The accuracy of these instruments was established and maintained in accordance with the calibration and standardization procedures described in detail in Appendix B of this report. Briefly, this consisted of initial certification of each instrument by the Douglas Aircraft Company metrology group and re-certification on a regular basis. Operating accuracy was checked on a day-to-day basis using a voltage standard accurate to ± 0.001 volt (9) which in turn was verified against a Weston Standard Cell whose accuracy is traceable to the National Bureau of Standards.

Inspection and quality control testing of sintered separators included measurement of porosity, permeability and transverse strength and careful visual examination, binocular microscope examination at 20x magnification and visual examination using transmitted light. Dimensional inspection consisted of measuring the thickness of each separator at the midpoint and at 4 points at 90° intervals around the outside of the separator in order to evaluate taper, flatness and parallelity.

Table II shows the thickness and porosity for a typical lot of No. 5-036-011 separators

These data indicate an acceptable level of uniformity with an average porosity of 12.39% and a standard deviation of ± 0.25%. The maximum spread of the porosity data between high and low values is 1.63%. As the accuracy of water absorption measurements of porosity in this range is probably not better than about 0.5%, the maximum variation is not greater than ± 0.5%.

The thickness data shown in Table II show dimensional uniformity of ± 0.0015 in. for a given sample and ± 0.002 in. maximum variation in the 50 dimensions measured in the group of 10 samples. These results indicate that careful process control makes it possible to fabricate inorganic separators to a high level of quality and uniformity. Further process improvement and separator fabrication on a larger scale during the course of contract NAS 3-7636 should result in additional substantial improvement of separator quality and uniformity.

TABLE II

THICKNESS AND POROSITY OF NO. 5-036-011 SEPARATORS LOT 01851-18

Sample Number	Thickness (in.)					Porosity (%)
	(1)	(2)	(3)	(4)	(5)	
1	0.012	0.014	0.014	0.012	0.015	12.66
2	015	015	015	012	015	12.65
3	015	013	014	013	013	12.81
4	016	015	016	014	015	12.62
5	014	014	011	015	014	12.51
6	013	016	013	015	013	11.81
7	015	014	015	013	014	12.71
8	015	013	015	014	015	13.47
9	013	015	013	015	013	11.48
10	015	014	015	014	015	11.18

Standard Deviation:

$\bar{X} = 12.39\% \pm 0.25$

2.2 Electrodes

2.2.1 Electrochemical Reaction Processes

Along with affording a high level of energy density, the silver-zinc system is characterized by such favorable operational characteristics as constancy of voltage level during discharge, relatively high hydrogen and oxygen overvoltages and a reasonable amount of chemical inertness in alkaline solutions.

The reactions for the silver-zinc cell, as they are generally recognized occur in two steps, involving "plus"-one and "plus"-two silver oxidation stages. These correspond to the characteristic lower and upper voltage plateaus, respectively, observed during charging and discharging regimes. The following equations describe these reactions:

Upper Voltage Plateau; Lower Voltage Plateau

$$2\,AgO + Zn + H_2O \quad \underset{\text{charge}}{\overset{\text{discharge}}{\rightleftarrows}} \quad \begin{array}{c} Ag_2O + Zn\,(OH)_2 \\ \updownarrows \\ ZnO + H_2O \end{array} \qquad (2)$$

$$Ag_2O + Zn + H_2O \quad \underset{\text{charge}}{\overset{\text{discharge}}{\rightleftarrows}} \quad \begin{array}{c} 2\,Ag + Zn\,(OH)_2 \\ \updownarrows \\ ZnO + H_2O \end{array} \qquad (3)$$

How the potentials are established in 30% KOH-aqueous solution at 25°C can be described by following sequence of equations.

(a) Equilibrium Potential of the Zinc Electrode

$$Zn\,(OH)_2 + 2\,OH^- \rightleftarrows ZnO_2^{=} + 2\,HOH \qquad (4)$$

$$ZnO_2^{=} + 2\,HOH + 2e \rightleftarrows Zn + 4\,OH^- \qquad (5)$$

$$Zn(OH)_2 + 2e \rightleftarrows Zn + 2\,OH^- \qquad (6)$$

or

$$ZnO + HOH + 2e \rightleftarrows Zn + 2\,OH^- \qquad (6a)$$

Equation (6) represents the overall reaction for electron transfer involving the zinc electrode. The potential resulting therefrom can be expressed in terms of the Nernst equation as follows:

$$\pi_{Zn} = \pi^{o}_{Zn} + 0.0592 \log \frac{1}{f_1 (OH)^-} \qquad (7)$$

wherein $\pi^{o}\, Z_n$ is the standard potential of the zinc electrode = - 1.245 volts; f_1 is the activity coefficient of OH^- ~2.14 (10) and (OH^-) is the molality of OH^- ions = 7.65 (for 30% KOH solution).

Substitution into Equation (7) yields the following potential for the zinc electrode, $\pi_{Zn} = 1.317$ volts (8)

(b) Equilibrium Potential of the Ag-Ag_2O Electrode

$$2\ Ag + 2\ OH^- \rightleftarrows Ag_2O + HOH + 2e \qquad (9)$$

Equation (9) represents the overall reaction for electron transfer involving the Ag-Ag_2O electrode. Substitution into the Nernst equation gives

$$\pi_{Ag}{}^{+} = \pi^{o}_{Ag}{}^{+} + 0.0592 \log \frac{1}{f_1 (OH)^-} \qquad (10)$$

wherein $\pi^{o}\, Ag^{+}$ is the standard potential of the Ag-Ag_2O electrode = + 0.344 volts. Therefore

$$\pi_{Ag}{}^{+} = 0.344 - 0.072 = 0.272 \text{ volts} \qquad (11)$$

(c) Equilibrium Potential of the Ag_2O - AgO Electrode

$$Ag_2O + 2\ OH^- \rightleftarrows 2\ AgO + HOH + 2e \qquad (12)$$

Substitution into the Nernst equation gives

$$\pi_{Ag}{}^{++} = \pi^{o}_{Ag}{}^{++} - 0.059 \log \frac{1}{f_1 (OH)^-} \qquad (13)$$

wherein $\pi^{o}_{Ag}{}^{++}$ is the standard potential of the Ag_2O-AgO electrode = 0.570 volts. Therefore

$$\pi_{Ag}{}^{++} = 0.570 - 0.072 = 0.498 \text{ volts} \qquad (14)$$

(d) Equilibrium EMF of the Silver-Zinc Cell When Fully Charged

Under such conditions, the positive electrode is AgO plus a small amount of Ag_2O and the negative electrode is Zn with some ZnO depending on the excess of zinc oxide originally present. The following are the pertinent reactions:

$$Ag + 2\ OH^- \rightleftarrows AgO + HOH + 2e \qquad (15)$$

$$ZnO + HOH + 2e \rightleftarrows Zn + 2\ OH^- \qquad (16)$$

$$Ag + ZnO \underset{\text{discharge}}{\overset{\text{charge}}{\rightleftarrows}} AgO + Zn \qquad (17)$$

Equation (17) is the overall equation for the process for which the equilibrium potential is E =

$$\pi_{Ag}{}^{+} + \pi Ag{+}{+} - \pi Zn = 0.272 + 0.498 - (-1.317)$$
$$= 2.087 \text{ volts} \qquad (18)$$

(e) EMF of the Silver-Zinc Cell on Discharge From The Upper Voltage Plateau

The positive electrode involved during the discharge from the upper voltage plateau involves the Ag_2O-AgO couple and Equations (13) and (7) can serve as the means for calculating the voltage of the cell as follows. During discharge, the hydroxyl ion concentration at the zinc electrode is lower than that in the bulk of the electrolyte (Equation 5 proceeding to the left). At the Ag_2O-AgO electrode, the hydroxyl ion concentration increases (Equation 12 proceeding to the left). By designating the hydroxyl ion concentration at the zinc electrode as $(OH)_n^-$ and that at the silver electrode as $(OH)_p^-$, the voltage of the cell on discharge becomes

$$E = \pi_{Ag}{}^{++} - \pi Zn \qquad (19)$$

Substituting Equation (13) for the silver electrode potential and Equation (7) for the zinc electrode,

$$\pi_{Ag}{}^{++} - \pi Zn = 0.570 - (-1.245) + 0.0592 \log \frac{f_1(OH)_n^-}{f_1(OH)_p^-} \qquad (20)$$

$$E = 1.815 + 0.0592 \log \frac{f_1 (OH)_n^-}{f_1 (OH)_p^-} \quad (21)$$

In this derivation, it is assumed that the activity coefficient for the hydroxyl ion remains the same for both compartments.

From Equation (21) it is apparent why the voltage drops below the equilibrium value (experimentally to as low as 1.6 volts), i.e., during discharge the hydroxyl ion concentration in the zinc compartment decreases while it increases in the silver compartment, rendering the logarithmic term negative. On the other hand, on charge, E becomes greater than the equilibrium value of 1.815 since $\frac{(OH)_n^-}{(OH)_p^-}$ becomes greater than unity. This fact is observed experimentally as voltages as high as 2.05 v are obtained.

In the development of these equations, unit activity was assumed for the concentration of water. Only a small error results thereby, especially since logarithmic terms are involved.

2.2.2 Characteristics of Silver-Zinc Electrodes and Their Preparation

(a) Silver Electrodes: Originally, in the late 1940's silver electrodes were made of pressed dry silver powder and were characterized by manifestations of structural weakness, relatively low density and relatively low electrical capacity (i.e., 6 - 8 g/ampere-hour).(10, 11) Improvements were effected, through the use of pasting and sintering techniques which will now be outlined.

In one process,(10) an aqueous paste of Ag_2O is spread over a grid; then, the plates are sintered, reducing the silver to the neutral state. The final stage involves oxidizing the silver to the "plus" two state by electrolytic (forming) methods. Similarly, the initial paste material could be AgO in water without any prior sintering and formation if only a primary battery is required.(11)

Sintering is most commonly used in current commercial practice. After sintering, electrolytic formation is resorted to prior to battery application. Sintered silver plates have been made at density levels of up to 4.5 g/cm^3. Several, different types of support materials have been used in connection with silver plates. In the earlier paste techniques, copper screen (mesh of 20 x 20 wires/cm) plated with nickel or silver were used. Next silver screen and finally expanded silver metal were used.

The method of making connections to the plates consisted of spot welding silver wire or strip into position, then pressing into the surface and finally the connection was firmly fixed by sintering. Forge welding of strips has been found to be highly effective, as well.

Silver plate materials for high rate cells involving sintered, expanded silver mesh and powder have yielded current capacities of the order of 2.5 to 3.5 g of 50/50 Ag/Ag_2O mixture per ampere-hour. This represents "electrode capacity efficiencies" based on actual capacity divided by theoretical capacity of 60 - 84%.

The silver electrode is highly sensitive to electrolyte deficiency during charging, which could be the controlling factor in cell behavior. Lack of electrolyte and limited diffusion impedes the extent to which the silver electrode can be charged, as is shown by Equations (9) and (10), above. Thereby, the discharge process is limited as well. In silver-zinc cells, the silver electrode potential governs the termination of charge.

There are a number of unexplained and complicating phenomena occurring during charge-discharge cycles involving the silver electrode, such as peroxide formation and the sudden disappearance of the upper voltage plateau during discharge. In addition, silver oxides are soluble to some extent in caustic solution.

(b) Zinc Electrodes: Zinc electrodes were first made by pasting a mixture of zinc oxide and potassium hydroxide onto a suitable grid.(10, 11) Such electrodes were fragile and afforded erratic behavior during formation. Currently, the general procedure is to press dry zinc oxide to grids in molds of the desired plate dimensions. Then, the electrodes are transferred to suitable containers and electrolytically formed to the zinc state. Plates made from powdered metallic zinc, although manifesting high density do not exhibit good electrical properties, probably because of a lack of porosity.

Another method of making active zinc electrodes is by electroplating on to a suitable matrix from either a cyanide solution or from a slurry of zinc oxide in alkaline solution. The plates are finally pressed to the required thickness. Ordinarily, zinc plates are made up to twice the thickness of silver plates, the latter ranging from 0.25 to 0.4 mm. Needless to say, electrode porosity as well as thickness are related to performance with rates of charging and discharging guiding both aspects. Thin plates and high porosities are conducive to better efficiency at high discharge rates.

2.2.3 Electrode Fabrication Procedures Used During Contract NAS 3-6007

The objective of this program was to establish the means for significantly improving the cycle life of silver-zinc batteries both at 25°C and at 100°C. The approach to these goals has been through the use of inorganic separators along with accompanying electrode development based on previous high energy density battery work done by Douglas.(4, 5, 6)

Initially, the contract specifications called for a test cell capacity of 0.9 ampere-hours. However, in Technical Directive No. 1, dated 28 August 1964, testing of 0.5 - 0.6 ampere-hour cells was approved in order to correlate these data with results previously obtained.

Electrodes prepared during this program have demonstrated capacity levels of the order of 0.38 ampere-hour per gram of silver in single compartment silver-zinc test cells. As cycle life was of paramount importance preparation techniques and test procedure were directed to this goal and relatively little attention was given to E. C. E. (electrode capacity efficiency). Nickel grids were used as electrode support materials throughout most of this investigation. Foam nickel metal matrices were used to a lesser extent. The use of silver support material was instituted during the latter stages after long cycle life had been achieved and more emphasis was then placed on E. C. E.

In this work the electrodes were prepared within the test cell compartment. A photograph of the individual compartments is shown in Figure 9. Figure 10 is a drawing of the test cell showing the dimensions used. These cells were machined from ceramically filled Teflon or from Celcon.

2.2.3.1 Silver Electrodes - Type A

This type of electrode was most frequently used during the program. It was prepared from a paste composed of 3 grams of

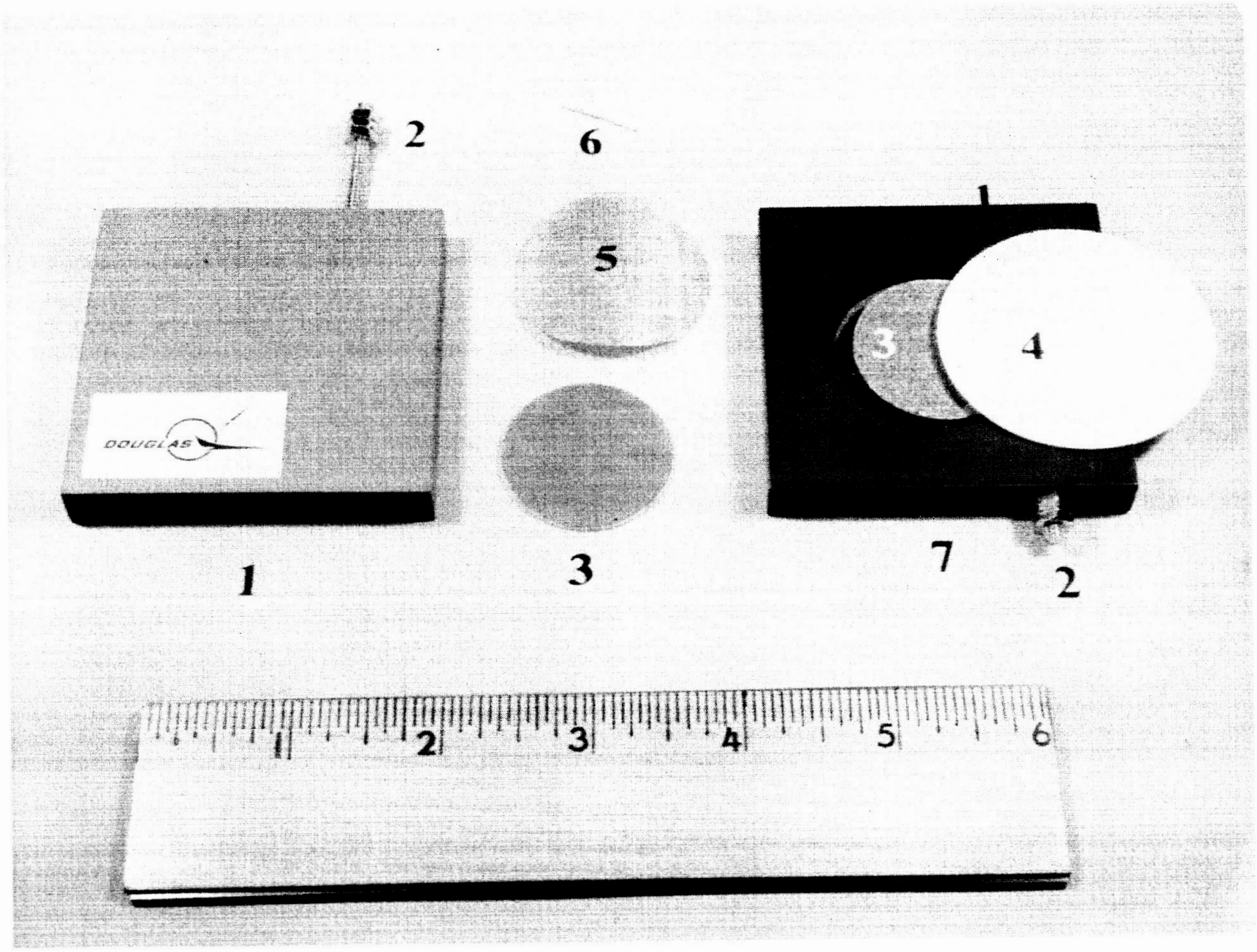

C1067

Figure 9. Demonstration Test Cell

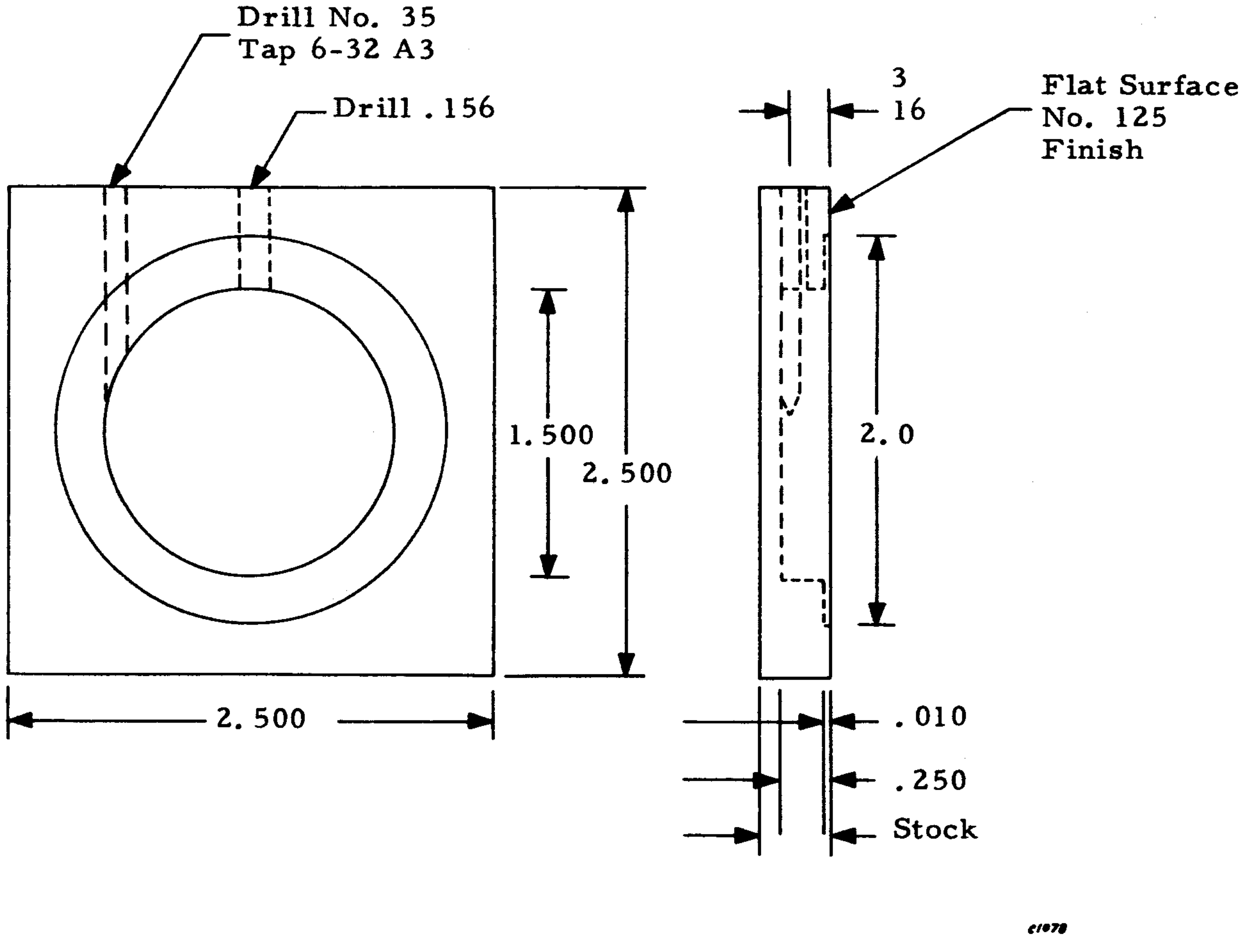

Figure 10. Test Cell

50/50 Ag-Ag_2O mixture made by adding about 3-4 ml of 30% KOH solution. A silver wire lead, 0.032-in diameter, was silver-soldered to a circular 1.5 in diameter, 200-mesh nickel screen. The circular grid was placed in the cell compartment and the silver wire lead passed through the top of the case as is shown in Figure 9. During the latter part of this program, it was found that resistance welding nickel wire to the nickel screen could also be used. This method is shown in Figure 11.

The cell compartment containing the electrode paste was then placed in a horizontal position on a vibration table and then flowed into place.

2.2.3.2 Zinc Electrodes - Type A

Zinc electrodes were prepared in a similar manner using the following materials:

ZnO	-	4.4 to 9.0 g
HgO	-	0.1 to 0.5 g
PVA	-	0.1 to 0.3 g

2.2.3.3 Silver Electrodes - Type B

Prepared as described under (A) except that a nickel metal matrix was used (Figure 12) in place of the nickel screen.

2.2.3.4 Zinc Electrodes - Type B

Prepared as described under (A) except that a nickel metal matrix was used (Figure 12) in place of the nickel screen.

2.2.3.5 Silver Electrodes - Type C

These electrodes were prepared in the following manner:

Three grams of 50/50 Ag-Ag_2O mixture was placed on a nickel screen located in the electrode cavity. Then, a 1 - 1/2 in. male die was placed on top of the mix and pressed at 2 tons for approximately 15 seconds. After pressing, a 1-1/2 in. diameter NSM (Network Support Matrix) disc was placed on top of the electrode and pressed into the electrode surface.

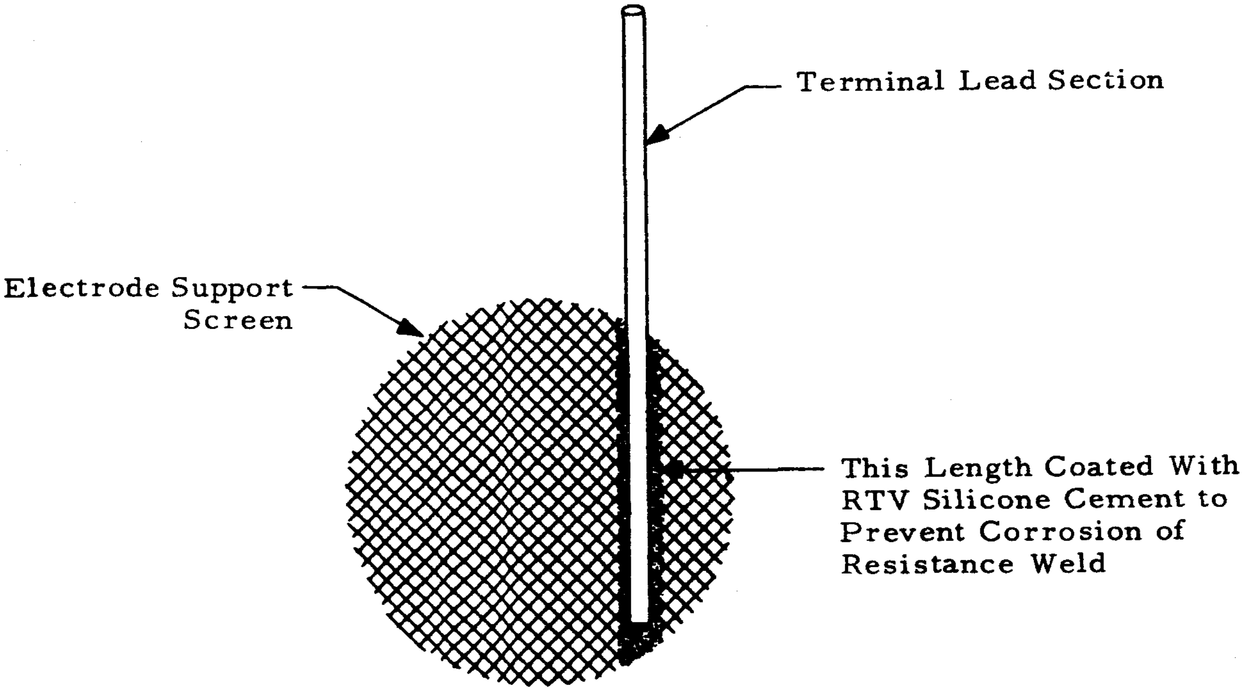

Material

200 Mesh Pure Nickel Screen

20 Gauge Pure Nickel or
Silver Wire

Figure 11. Electrode Current Collector Design

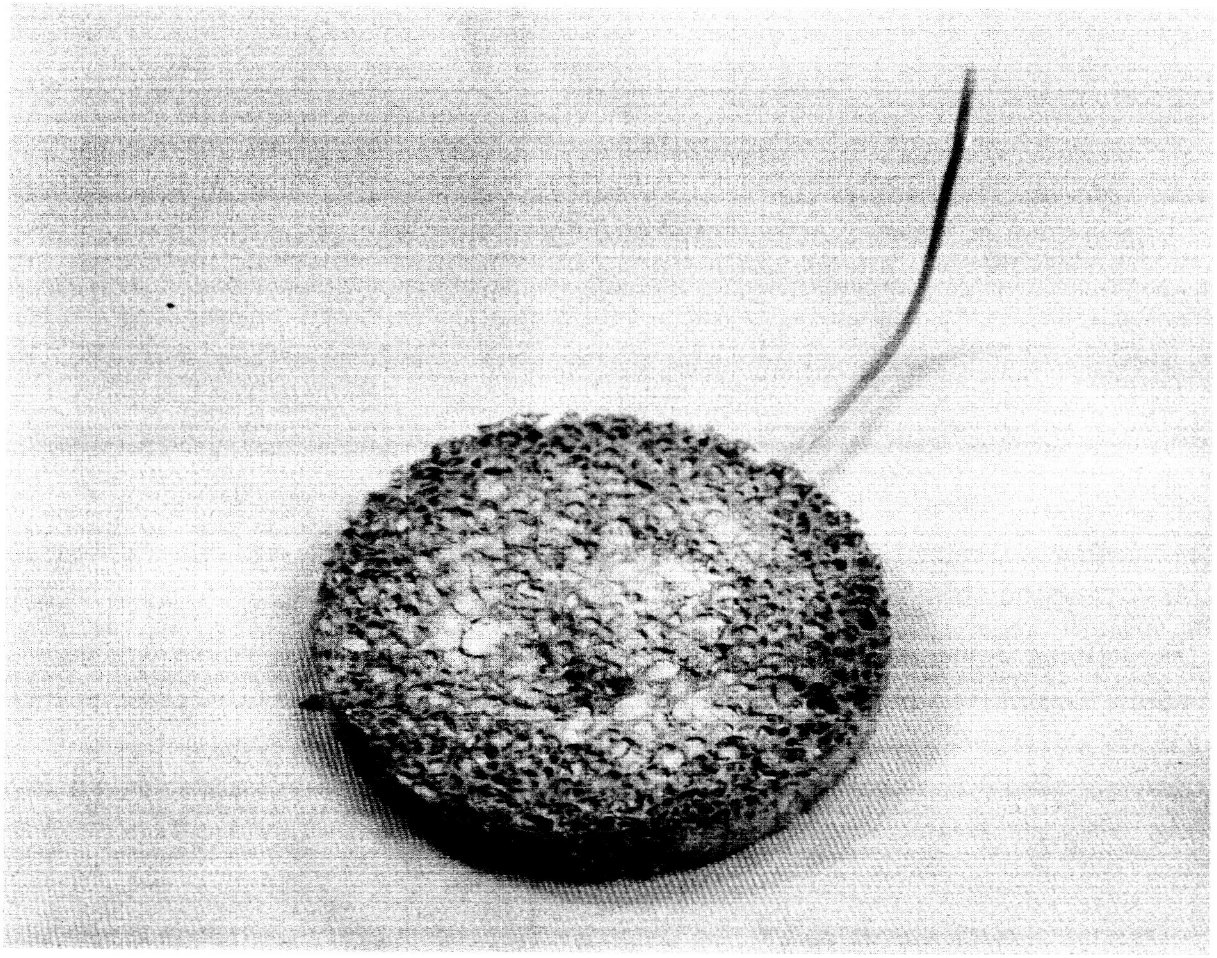

C1061

Figure 12. Special Paste Electrode Prepared in Conducting Matrix

2.2.3.6 Zinc Electrodes - Type C

This was also a pressed electrode and was prepared as follows:

7.5 g of zinc oxide mercuric oxide and PVA (90.3%, 5.2% and 4.5% respectively) was placed on top of the nickel screen located in the electrode cavity and pressed using a 1-1/2 inch die at 2 tons for approximately 15 seconds. After removal of the assembly from the press, a 1-1/2 inch diameter NSM disc was placed on the mix and hand-pressed into the electrode.

2.2.3.7 Silver Electrodes - Type D

These sintered electrodes were prepared in the following manner:

A 10-14 g of 50/50 Ag-Ag_2O mixture were compacted in a two inch die at 10-20 tons pressure. The discs were then sintered at 300°C for 1-1-1/2 hours. After sintering, the discs were cut to fit the electrode compartment and nickel screens were tack-welded to them.

Figure 5 shows the cell casings used in this work.

2.2.4 Electrode Materials Used in NAS 3-6007 Program

The following materials were used for electrode fabrication:

(a) Silver Powder: Types A, B and D electrodes involved Mallinckrodt Analytical Grade Precipitated Powder No. 2118 in their preparation. Type C electrodes were made from Handy-Harman Silpower No. 130. This silver has a much finer particle size than the former. Handy-Harman Silpower No. 130 is certified to be in the 0.6-3.0 micron range while the Mallinckrodt silver has a particle size ranging from 40 to 800 microns.

(b) Silver Oxide: Mallinckrodt Purified Powder No. 218

(c) Zinc Oxide: Mallinckrodt Analytical Grade No. 1426

(d) Polyvinyl Alcohol: duPont Grade 51-05

2.2.5 Electrode Formation Procedures

After assembly, the cells were vacuum-filled with 30% KOH solution and formed according to the following schedule:

Step 1: Charge at 25°C at 100 ma constant current for the 15 hours. The cell voltage should be 2.05 ± 0.05 volts and open circuit voltage 1.84 ± 0.04 volts before proceeding to Step 2.

Step 2: Discharge at 25°C at 100 ma constant current to 0.9 volt.

Step 3: Charge as in Step 1.

Step 4: Discharge as in Step 2.

Step 5: Charge as in Step 1. After completion of Step 5, the cell is ready for testing.

3.0 EXPERIMENTAL RESULTS

3.1 Test Cell Design

The test cell cases were machined from stock plates of a ceramically filled Teflon.* The gasketing material used was virgin Teflon, Type TFE. Figure 13 shows an exploded view of a test cell consisting of two Teflon case halves (one positive electrode case and one negative electrode case), two fluorocarbon gaskets, the electrodes, and the Astroset inorganic separator. Figure 14 is a view of a fully assembled test cell.

Difficulty was encountered during the initial phase of the contract with leakage of electrolyte from the cell case assembly following several hundred cycles at 25° or 100°C. Investigation showed that the cementing of Teflon gaskets to the cell cases was inadequate due to poor adherence of the cement to the Teflon gasketing material. A design improvement was instituted, involving the introduction of gasket material made from ceramic-filled fluorocarbon, which was cut from sheet stock to match the dimensions of the cell cases. This gasket material was pretreated so it could be bonded to the case halves by cementing and curing at room temperature. The new gasket produced produced an improved seal between the cell case halves and minimized case leakage at both room temperature and 100°C.

The test cells fabricated throughout the first half of the contract utilized the electrode current collector design shown in Figure 11. In this design silver wire was silver-soldered to the nickel support screen and the active electrode material was impregnated into the screen. Repeated cycling test cells incorporating this current collector design, caused corrosion of the silver-solder after several hundred cycles with eventual loss of contact between the silver wire and the nickel screen. Several test cells were removed from the cycling programs due to this wire failure. The fabrication method was then changed to welding the silver lead wire to the nickel support screen. The welded area was coated with RTV silicone cement to prevent electrochemical corrosion of the weld during the cycle testing. This assembly performed considerably better than the silver-soldered type, however, the RTV coating was eventually chemically attacked by the hot electrolyte and resulted in contamination of the electrolyte. In several other test cells, the silver wire was replaced with

---

*TECfluorofil, Grade BF-1, Thermech Engineering Corporation, Anaheim, Calif.

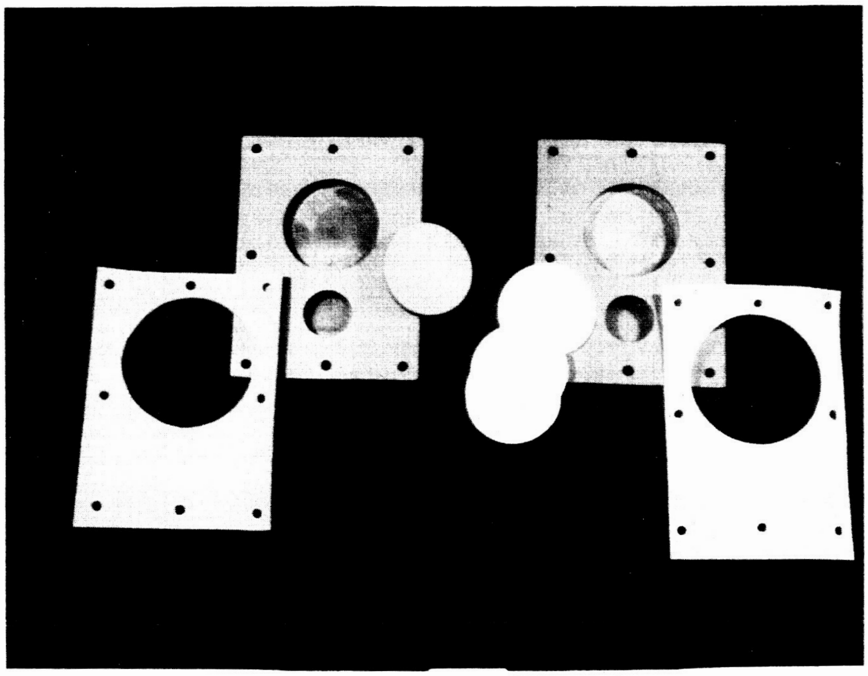

Figure 13. Exploded View Showing Test Cell Components

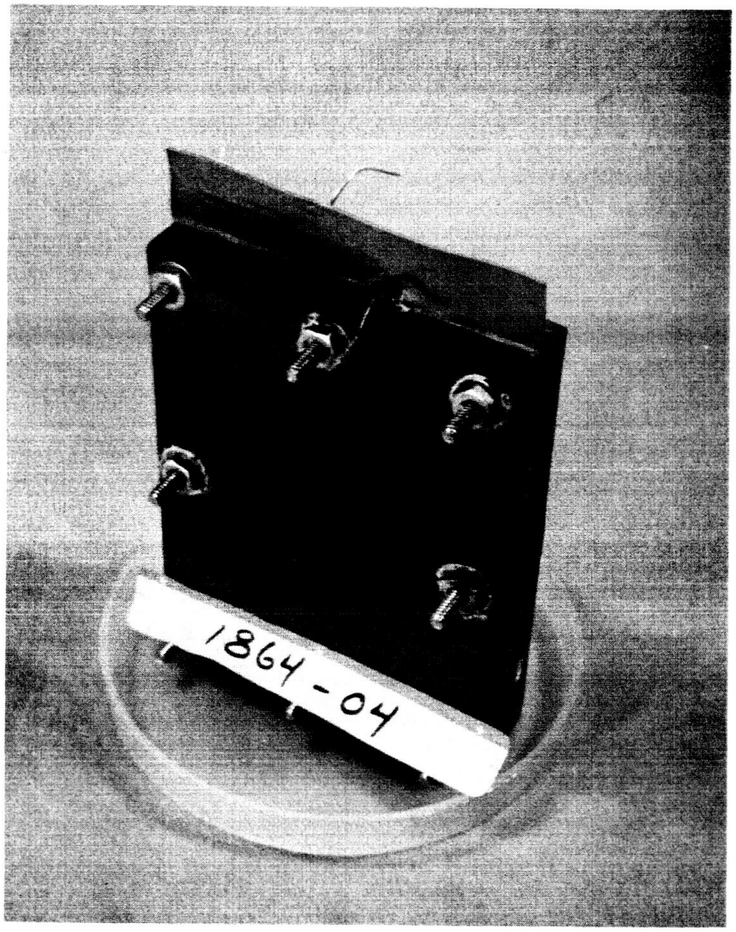

Figure 14. Silver-Zinc Test Cell

a nickel wire, resistance welded to the nickel collector screen. This did not, however, improve the operational performance of the test cell on cycling and these tests were discontinued.

As a result of cycle testing a large number of test cells, it became apparent that cell failure usually resulted from detachment of the terminal lead wire from the electrode collector screen. When this occurred, it was usually impossible to re-establish electrical contact with the electrode, and, the test had to be discontinued, even though, the electrodes and separators were capable of many additional cycles.

This problem was discussed during the conference held at Astropower Laboratory on February 17, 18, 1965, with the NASA Project Officers. Several worthwhile suggestions resulted from this conference, which included:

1. Use of a silver foil or screen as a current collector and terminal connector wire.
2. Elimination of the use of silver alloys for joining terminal wires to collector screens.
3. Coating the welded section between the terminal lead wire and the collector screen with a suitable protective plastic which is not attacked by hot KOH.
4. Investigation of the use of chemically inert solders such as germanium-gold for joining the terminal wire to the collector screen.

As a result of these suggestions several new designs were incorporated into test cells. One design used a 200 mesh nickel screen cut to the shape of the circular electrode with a tab extending from the screen to serve as the terminal lead, (Figure 15). The upper portion of the terminal lead was impregnated with RTV silicone cement to prevent the wicking of the electrolyte. Test Cell Nos. 1873-003 and 1849-040 were assembled with this current collector assembly design and cycled at 100°C. These test cells successfully completed 720 and 768 cycles, respectively, without any noticeable degradation in the condition of the screen assembly. The demonstration test cells described in Section 3.2.5 of this report also contained current collector screen assemblies of this design, except that the assembly was made with silver mesh, rather than nickel.

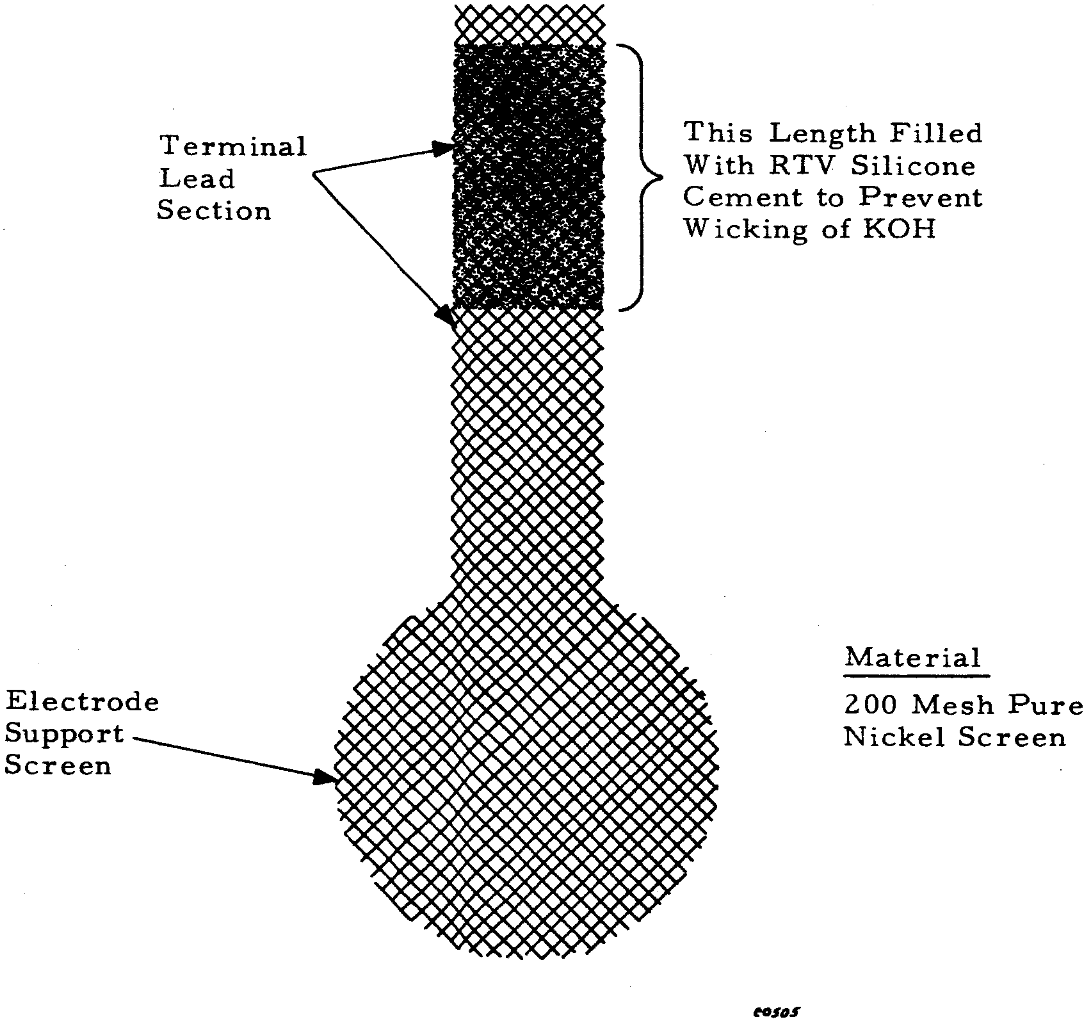

Figure 15. Nickel Mesh Terminal Lead Wire and Electrode Support Screen Assembly

Another design was incorporated into Test Cell No. 1911-010 to establish the effects of deep depths of discharge on cell performance, as well as the effects on solid silver collector sheets. Figure 16 is a drawing of this assembly design consisting of a 0.005 inch thick pure silver sheet formed into the circular configuration of the electrode, with an extension serving as the terminal lead section. The active electrode material was compacted in the dry state on both sides of the silver foil. This cell successfully completed 43 consecutive 100% charge-discharge cycles at room temperature without noticeable effect on the collector assembly.

The electrode-current collector design shown in Figure 17 was also evaluated. In this configuration, the terminal wire is preformed into a multiple "S" shape, and the shaped wire is placed in the electrode compacting die. Active electrode material is placed both under and on top of the shaped wire and compacted at high pressure forming an integrated current collector, electrode, and terminal wire assembly. The "S" configuration of the pre-formed electrode wire greatly increased the contact area between the current collector-terminal wire and the electrode active material as well as increasing mechanical strength and physical ruggedness. Test Cell No. 1911-040 was prepared using this design and was cycled at 25°C. The cell successfully completed 758 cycles without deterioration.

3.2 Cell Testing

3.2.1 Electrode Evaluation

The most significant electrode cycle test results obtained in this program are summarized in Tables III through VIII. These tests are arranged according to the types of electrodes used (i.e., A. B. C, and D)* and test temperatures (i.e., 25° and 100°C).

Cycling was carried out at approximately 20% depth of discharge after the electrodes had been formed at 25°C. Normally, charging current density was 12 ma/cm^2 and the discharge current density was 20 ma/cm^2 based on the effective electrode cross-sectional area of 10 cm^2.

The test results reported in Table III are an evaluation of Type A silver and zinc electrodes at 25°. A maximum life of 2704 cycles was

---

* Described in Section 2.2.3.

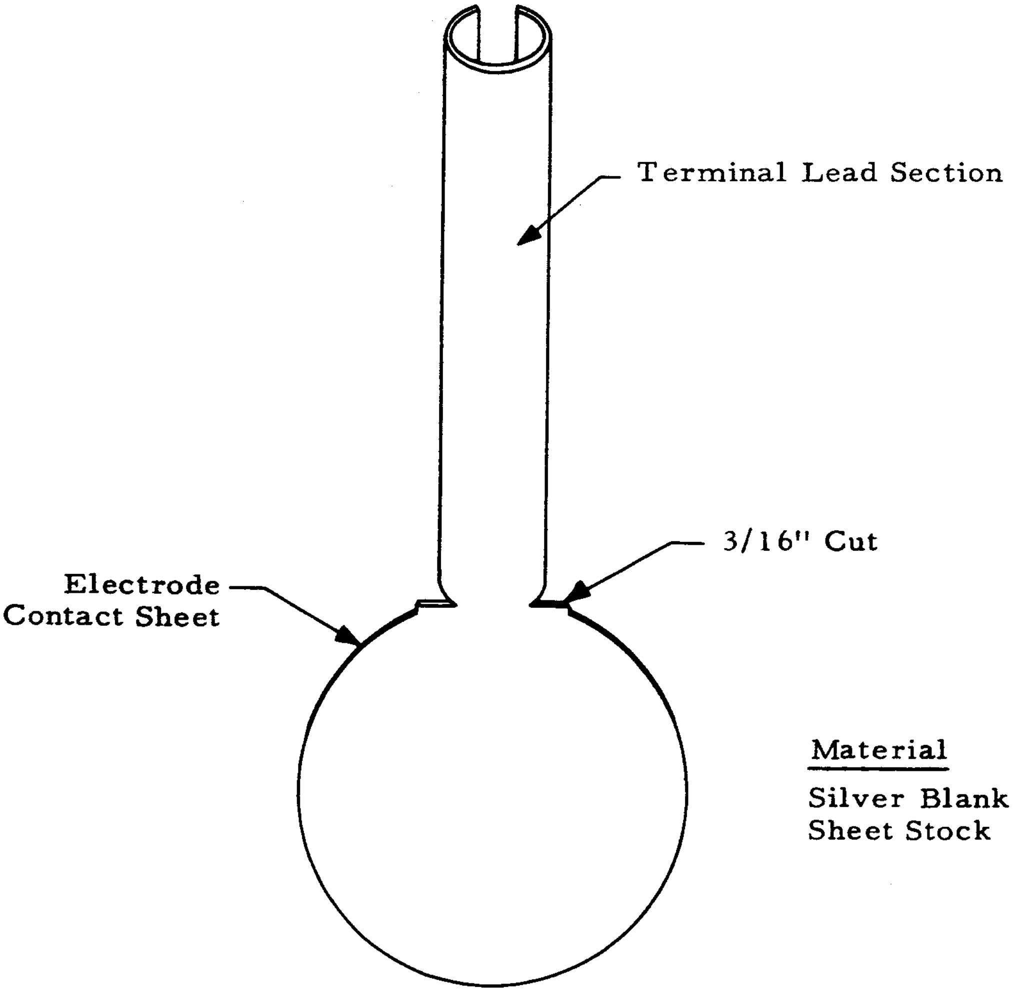

Figure 16. Silver Blank Electrode Terminal Lead Wire and Support Screen Assembly

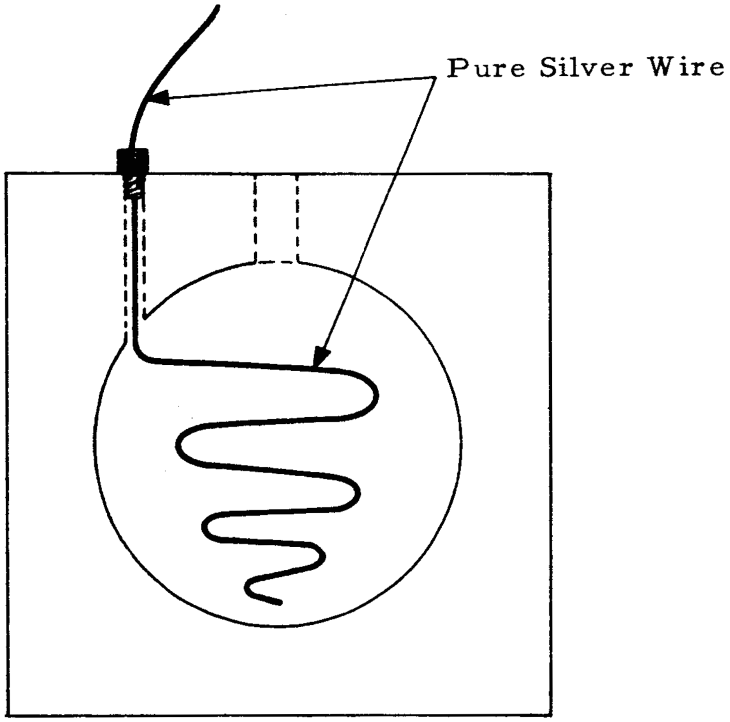

Figure 17. Single Terminal Lead Wire and Electrode Support

TABLE III

SUMMARY OF CYCLE LIFE TESTS PERFORMED WITH TYPE A SILVER AND ZINC ELECTRODES AT 25° C

Test No.	Cell Designation No.	Positive Electrode				Negative Electrode						Theor. AH Capa.	Cycling				Cycles Comp.
		Ag gms	Ag_2O gms	Ag %	Ag_2O %	ZnO gms	HgO gms	PVA gms	ZnO %	HgO %	PVA %		Discharge Hrs	Discharge Ma	Charge Hrs	Charge Ma	
1	88-95	1.5	1.5	50	50	4.36	0.12	0.02	97.0	2.67	0.3	1.44	0.5	200	1.0	120	2116
2	177-30	1.5	1.5	50	50	6.77	0.39	0.34	90.3	5.2	4.5	1.44	0.5	200	1.0	120	2704
3	177-80	1.5	1.5	50	50	6.77	0.39	0.34	90.3	5.2	4.5	1.44	0.5	200	1.0	120	1228
4	168-55	3.0	3.0	50	50	5.82	0.16	0.02	97.0	2.7	0.3	2.88	0.5	200	1.0	120	912

TABLE IV

SUMMARY OF CYCLE LIFE TESTS PERFORMED WITH TYPE A SILVER AND ZINC ELECTRODES AT 100° C

Test No.	Cell Designation No.	Positive Electrode				Negative Electrode						Theor. AH Capa.	Cycling				Cycles Comp.
		Ag gms	Ag_2O gms	Ag %	Ag_2O %	ZnO gms	HgO gms	PVA gms	ZnO %	HgO %	PVA %		Discharge Hrs	Discharge Ma	Charge Hrs	Charge Ma	
5	1869-40	1.5	1.5	50	50	6.32	0.36	0.32	90.3	5.2	4.5	1.44	0.5	200	0.5	240	768
6	1894-10	1.5	1.5	50	50	6.77	0.39	0.34	90.3	5.2	4.5	1.44	0.5	100	1.0	60	1344
7	1873-03	1.5	1.5	50	50	6.77	0.39	0.34	90.3	5.2	4.5	1.44	0.5	150	0.5	160	720
8	177-91	1.5	1.5	50	50	6.77	0.39	0.34	90.3	5.2	4.5	1.44	0.5	200	0.5	240	1482
9	1865-10	1.5	1.5	50	50	6.77	0.39	0.34	90.3	5.2	4.5	1.44	0.5	200	1.0	120	880
10	1869-20	1.5	1.5	50	50	6.77	0.39	0.34	90.3	5.2	4.5	1.44	0.5	200	1.0	120	794
11	1873-24	1.5	1.5	50	50	6.77	0.39	0.34	90.3	5.2	4.5	1.44	0.5	200	1.0	120	1329
12	1865-40	1.5	1.5	50	50	8.30	0.43	0.27	92.2	4.8	3.0	1.44	0.5	200	1.0	120	1548
13	1893-30	1.5	1.5	50	50	9.03	0.52	0.45	90.3	5.2	4.5	1.44	0.5	200	0.5	210	836

TABLE V

SUMMARY OF CYCLE LIFE TESTS PERFORMED WITH TYPE D SILVER ELECTRODES AND TYPE A ZINC ELECTRODES AT 25°C

Test No.	Cell Designation No.	Positive Electrode				Negative Electrode						Theor. AH Capa.	Cycling				Cycles Comp.
		Ag gms	Ag_2O gms	Ag %	Ag_2O %	ZnO gms	HgO gms	PVA gms	ZnO %	HgO %	PVA %		Discharge Hrs	Discharge Ma	Charge Hrs	Charge Ma	
14	128-62	7.61	--	100	--	5.40	0.30	0.30	86.2	6.9	6.9	3.79	0.5	300	1.0	1.80	1022
15	143-01	7.61	--	100	--	5.40	0.30	0.30	86.2	6.9	6.9	3.79	0.5	300	0.5	3.60	668
16	152-30	7.61	--	100	--	5.51	0.31	0.18	91.8	5.2	3.00	3.79	0.5	300	1.0	1.80	466

TABLE VI

SUMMARY OF CYCLE LIFE TESTS PERFORMED WITH TYPE D SILVER ELECTRODES AND TYPE A ZINC ELECTRODES AT 100° C

Test No.	Cell Designation No.	Positive Electrode				Negative Electrode						Theor. AH Capa.	Cycling				Cycles Comp.
		Ag gms	Ag_2O gms	Ag %	Ag_2O %	ZnO gms	HgO gms	PVA gms	ZnO %	HgO %	PVA %		Discharge		Charge		
													Hrs	Ma	Hrs	Ma	
17	152-60	5.43	--	100	--	5.52	0.31	0.18	92.0	5.1	2.9	2.70	0.5	300	0.5	360	232
18	152-55	5.43	--	100	--	5.52	0.31	0.18	92.0	5.1	2.9	2.70	0.5	300	0.5	350	330
19	143-10	7.61	--	100	--	5.40	0.30	0.30	86.2	6.9	6.9	3.79	0.5	300	1.0	180	216

TABLE VII

SUMMARY OF CYCLE LIFE TESTS PERFORMED WITH TYPE C SILVER AND ZINC ELECTRODES

Test No.	Cell Designation No.	Positive Electrode				Negative Electrode						Theor. AH Capa.	Discharge		Charge		Cycles Comp.	Temp. °C
		Ag gms	Ag_2O gms	Ag %	Ag_2O %	ZnO gms	HgO gms	PVA gms	ZnO %	HgO %	PVA %		Hrs	Ma	Hrs	Ma		
20	1911-10	3.0	--	100	--	6.77	0.39	0.34	90.3	5.2	4.5	1.49	--	--	--	--	43 (100% depth of discharge)	25
21	1911-40	3.0	--	100	--	6.77	0.39	0.34	90.3	5.2	4.5	1.49	0.5	150	1.0	85	758	25
22	1911-50	3.0	--	100	--	6.77	0.39	0.34	90.3	5.2	4.5	1.49	0.5	200	0.5	220	1258	100

TABLE VIII

SUMMARY OF CYCLE LIFE TESTS PERFORMED WITH TYPE B SILVER AND ZINC ELECTRODES AT 25° C AND AT 100°C

Test No.	Cell Designation No.	Positive Electrode Ag gms	Ag$_2$O gms	Ag %	Ag$_2$O %	Negative Electrode ZnO gms	HgO gms	PVA gms	ZnO %	HgO %	PVA %	Theor. AH Capa.	Discharge Hrs	Discharge Ma	Charge Hrs	Charge Ma	Cycles Comp.	Temp. °C
23	1875-10	1.5	1.5	50	50	6.77	0.39	0.34	90.3	5.2	4.5	1.44	0.5	85	1.0	60	836	25
24	152-15	1.5	1.5	50	50	5.52	0.31	0.18	92.0	5.1	2.9	1.44	0.5	200	0.5	240	700	100
25	1868-33	1.5	1.5	50	50	6.77	0.39	0.34	90.3	5.2	4.5	1.44	0.5	200	0.5	240	278	100
26	1873-50	1.5	1.5	50	50	6.77	0.39	0.34	90.3	5.2	4.5	1.44	0.5	200	0.5	240	288	100
27	143-60	3.0	3.0	50	50	5.52	0.31	0.18	92.0	5.1	2.9	2.88	0.5	300	1.0	180	192	100
28	143-30	5.0	5.0	50	50	5.52	0.31	0.18	92.0	5.1	2.9	4.81	0.5	300	1.0	160	245	100

obtained in this group. The results shown in Table III indicate that the relative amounts of zinc oxide,2.84-4.46 ampere-hour of zinc to 1.44 ampere-hour of silver, mercuric oxide (3-5%) and PVA, (0.3-4.5%) are not critical, at these concentration levels. At the termination of each of these tests, the negative electrodes were significantly depleted. The silver electrodes and inorganic separators, in each case were in good condition and appeared to be capable of continued cycling. In fact, negative electrode depletion was the major cause for test termination in the electrode evaluations described in Tables III through VIII.

The results in Table IV were obtained with the same, Type A, electrodes at 100°C. Maximum cycle life as high as 1548 cycles was obtained over a one-hour charge, 1/2-hour discharge continuous cycling regime for approximately one half of these tests. Test 5, 7, 8 and 13 were performed on a 1/2-hour charge, 1/2-hour discharge cycling sequence. It does not appear that the shorter charging time, requiring doubling of the charging current density had an effect on cycle life.

The principal cause of failure appeared to be the depletion of the zinc electrode. Filling the negative compartment with more active electrode material as in Test 13 does not appear to enhance cycle life.

The results in Table V were performed with sintered silver electrodes (Type D) and Type A zinc electrode. Although there are some significant variations in test conditions compared with those in Table I, it must be concluded at this point that the use of sintered silver electrodes does not offer any particular advantages over the paste type.

It can be seen from Table IV that the sintered silver electrodes do not perform as well at 100°C as at 25°C. However, in the program continuation the effect of sintering conditions such as temperature level and time, will be covered. Undoubtedly, both affect surface structure and porosity and hence, electrode passivation.

Type C silver (100% Ag) and zinc electrodes according to the results of Table V show promise, especially at 100°C. Such electrodes appear to resemble commercial-type electrodes in physical appearance. It is planned to continue to explore the advantages of this mode of fabrication of electrodes in this new program.

As shown in Table VIII silver and zinc supported on nickel matrix (Type B) electrodes do not show as much promise as the paste (Type A) and pressed (Type C) electrodes. This type of electrode structure will not be used in forthcoming efforts with the Astropower inorganic separator. In addition, it is recognized that nickel matrices afford disadvantages from a conductivity limitation as well as from sufficient electrochemical activity with zinc to be conducive to gassing tendencies. Substitution of silver material for nickel should result in significantly better performance hereafter.

Since the most direct cause of failure in the tests described in Tables III through VIII appeared to be the depletion of zinc electrode, it would be appropriate at this time to relate our observations to discussions on this matter found in the literature.

Passivated zinc consists of a layer of zinc oxide with small amounts of gamma Zn $(OH)_2$, according to Hampson, Tarbox and Lilly(12). According to Young(13), zinc in the passive state acquires an inner coat of oxide material, probably ZnO but not Zn $(OH)_2$. The latter persumably forms the outer coat. The inner film can exhibit various colors such as yellow brown, violet-black, grey-violet, and blue black. According to Huber(14), these colors are not interference colors but actually due to particles of zinc distributed throughout the zinc oxide.

It is reported in the literature that zinc electrodes have been observed which show color variations ranging from white at the back to from grey to blue facing the separator. The experiments of Hampton, Tarbox and Lilly(12) indicate that when a zinc anode is allowed to remain at rest for a short period of 'time, it will become depassivated. However, the time required for re-passivation is always shorter than for an electrode not previously passivated. Related discussions on the matter are given in References 15, 16, and 17.

In the tests described in Table I through VI, inclusive, the zinc electrodes after disassembly of the cells have been found to show colors ranging from dark grey to light grey, and dark-blue to bright blue. For the most part, these cells had been cycled at currents in the 100-200 ma range. It appeared that when higher cycling currents were used, the dark color pattern became more complex; there were signs of earlier and more extensive passivation of the zinc. The same indication existed after longer cycling periods at the lower current levels.

3.2.2 Cycle Testing

The major objective of this program was to develop test cells based on Astroset 5-036-011 inorganic separators and electrode configurations which were capable of 1500 discharge-charge cycles at 100°C. These cells were also to be evaluated at 25°C, 125° and 150°C in order to define the problems associated with this approach to high energy density silver-zinc configurations.

3.2.2.1 Cycle Testing at 100°C

Cycle testing was performed for the purpose of determining the cycle capability of silver-zinc cells consisting of Astroset 5-036-011 inorganic separator and novel electrode configurations. Those cells which were capable of being continuously cycled at 100°C were permitted to cycle for 1500 cycles or until failure. As a result of this test program, several cells successfully completed the 1500 cycles at 100°C, thereby meeting the test goals of the work statement.

Although electrode development was not a prime objective of this program, several novel silver and zinc electrode formulations and configurations were cycled at 25°C and 100°C in test cells employing Astroset 5-036-011 inorganic separators.

As a result of the long cycle life attained with inorganic separators at 100°C, the principal reason for test termination was due to the deterioration of the zinc electrode. Although it is recognized that the zinc electrode is a limiting component in the silver-zinc system, the zinc electrode is not usually a prime cause of failure in commercial silver-zinc cells which are limited to ambient operating temperatures. In most cases the organic separators are the limiting factor which causes commercial cells to fail prior to the occurance of zinc electrode changes. As the test cells in this program were evaluated at 100°C and the inorganic separators were capable of long cycle life, deterioration of the zinc electrode became evident as the major reason for test termination. Although the work statement objective of 1500 cycles at 100°C was satisfactorily complied with, zinc electrode changes were usually evident after 800 to 1000 cycles.

Test Cell No. 1867-040, for example, completed

2,286 charge-discharge cycles at 100°C when it was removed from cycle test due to low open circuit voltage. Typical cycle test results for the 1000th and 2100th cycles are shown in Figure 18. Test Cell No. 1865-040 was also removed from 100°C cycle test after completing 1548 cycles because of low open circuit voltage. This cell also evidenced depletion of the zinc electrode. Figure 19 shows the charge-discharge voltage curves for the 1st, 856th, 1200th, and 1500th cycles.

Test Cell No. 177-091 was removed from 100°C cycle testing after 1482 cycles when the zinc electrode terminal lead wire had separated from the current collector screen. Cycle test results for the 1st, 259th, 1174th and 1464th cycle are shown in Figure 20. Other test cells which successfully completed prolonged cycling at 100°C were Test Cell No. 1911-050, which completed 1258 cycles, Test Cell No. 1894-010, which completed 1344 cycles, Test Cell No. 1873-024, which cycled for 1329 cycles, and Test Cell No. 177-060, which completed 1072 cycles. Figures 21 and 22 show charge-discharge cycle test curves for Test Cell No. 1911-050 and 1873-024, respectively.

Table IX shows the number of cycles obtained and the test conditions used for the test cells evaluated at 100°C. A number of other test cells were removed from 100°C cycle testing for various reasons other than electrode or separator problems. These reasons for test termination included cell case leakage, broken terminal wires, and test equipment malfunctions. For example, the silver electrode lead wire became loose in Test Cell No. 88-010, following the completion of approximately 300 cycles. The lead wire was then forced further into the electrode matrix in order to continue cycling. After an additional 69 cycles, the cell again became erratic and was disassembled. It was found that the lead wire had broken away from the grid, apparently due to stress exerted on the lead wire by the test leads.

As discussed in a previous section of this report, electrode lead wire design improvements were incorporated in test cells which were fabricated later on in the program. These designs proved to be successful and permitted extended cycling at 100°C.

In the case of Test Cell No. 169-035, 211 cycles were completed at 100°C when trouble developed with the sand bath temperature controller and the test temperature rose above 150°C. Upon disassembly of the

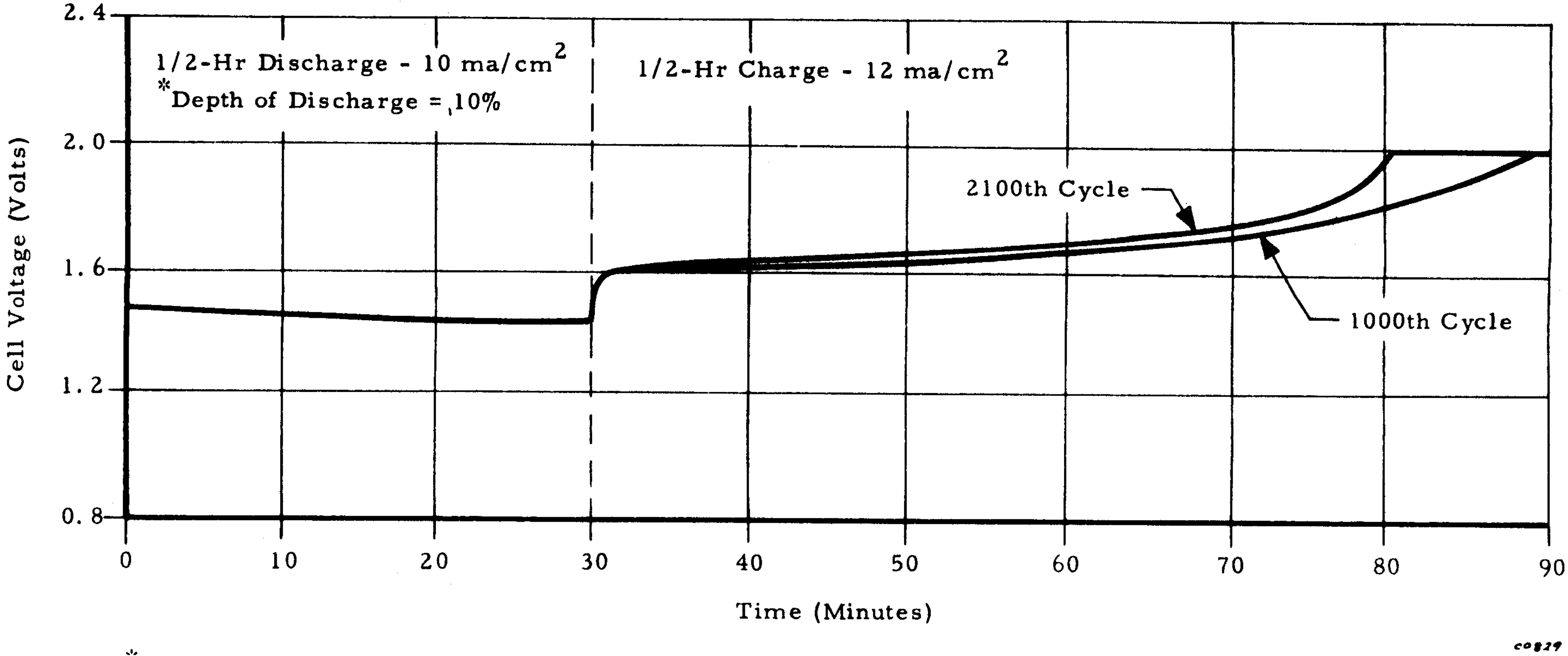

*Based on low rate capacity (16 hr discharge)

Figure 18. Test Cell No. 1867-040 Charge-Discharge Cycle Test Curves at 100° C

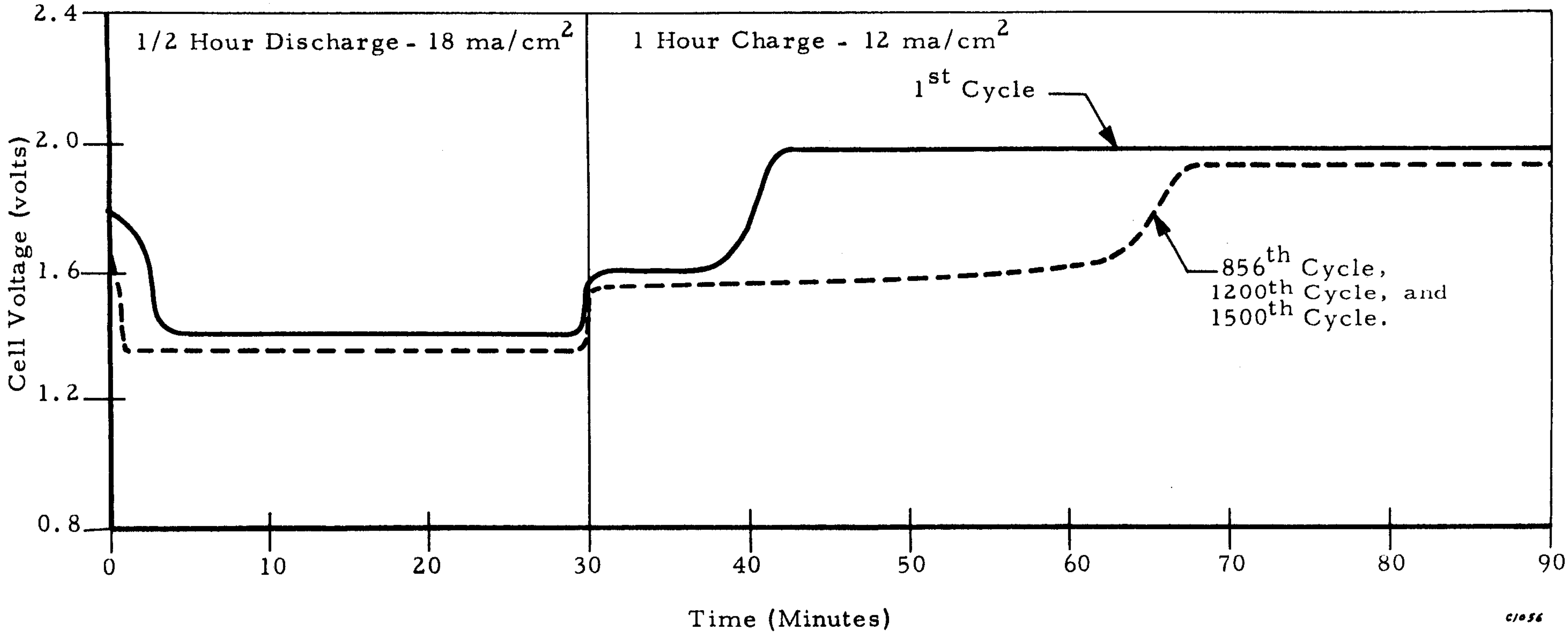

*Based on low rate capacity (16 hour discharge)

Figure 19. Test Cell No. 1865-040 Charge-Discharge Cycle Test Curves at 100° C

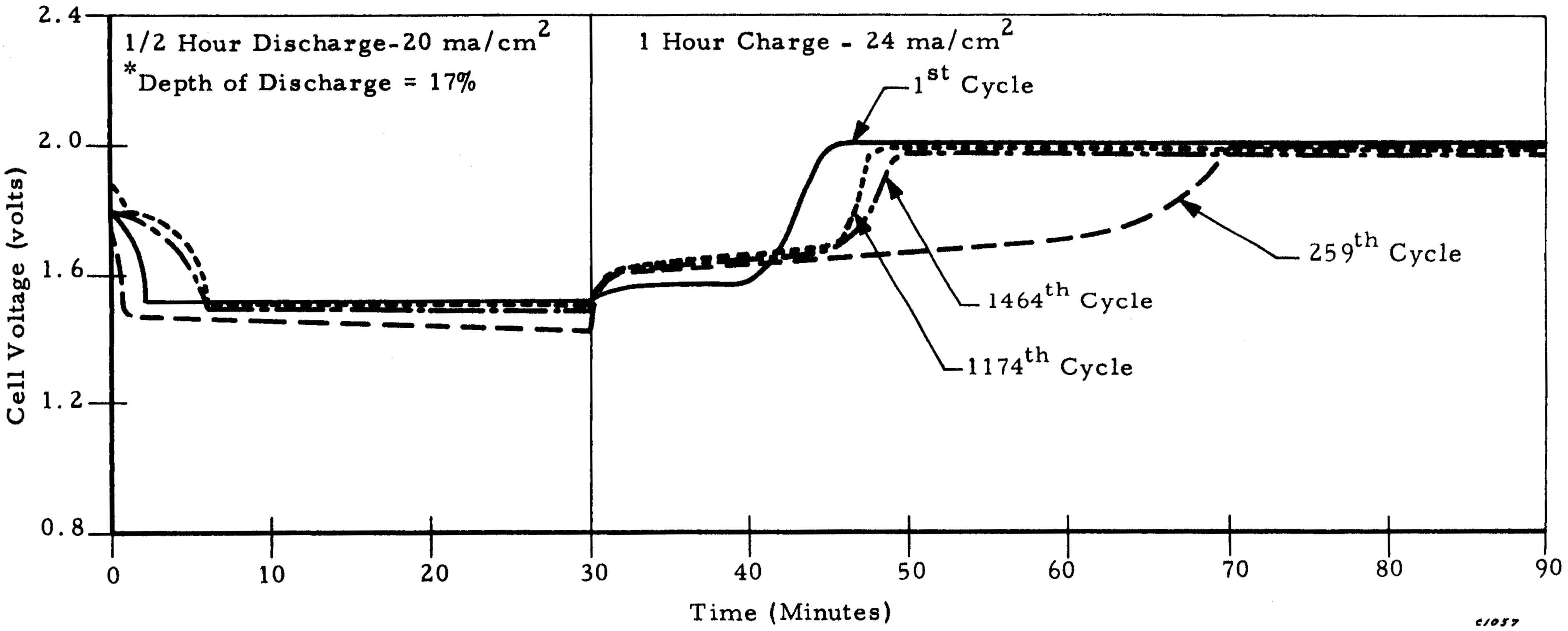

*Based on low rate capacity (16 hour discharge)

Figure 20. Test Cell No. 177-091 Charge-Discharge Cycle Test Curves at 100° C

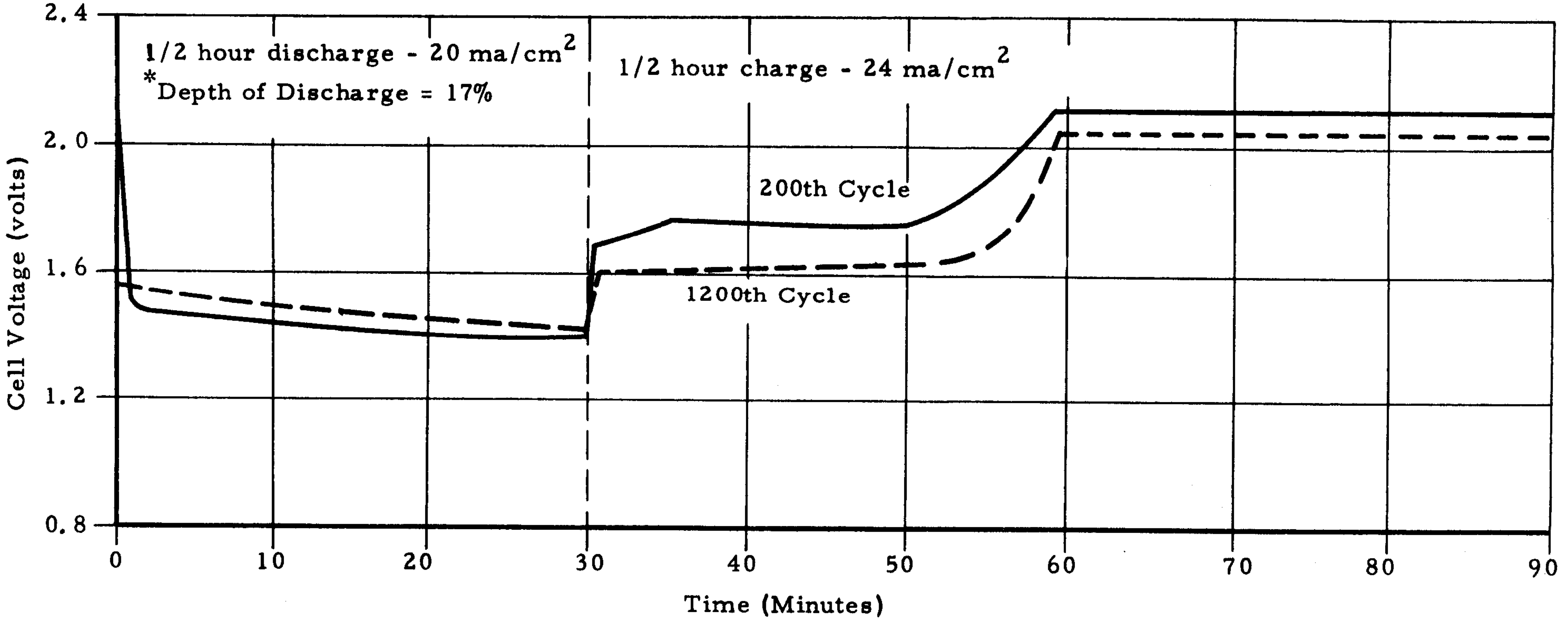

*Based on low rate capacity (16 hour discharge)

Figure 21. Test Cell No. 1911-050 Charge-Discharge Cycle Test Curves at 100° C

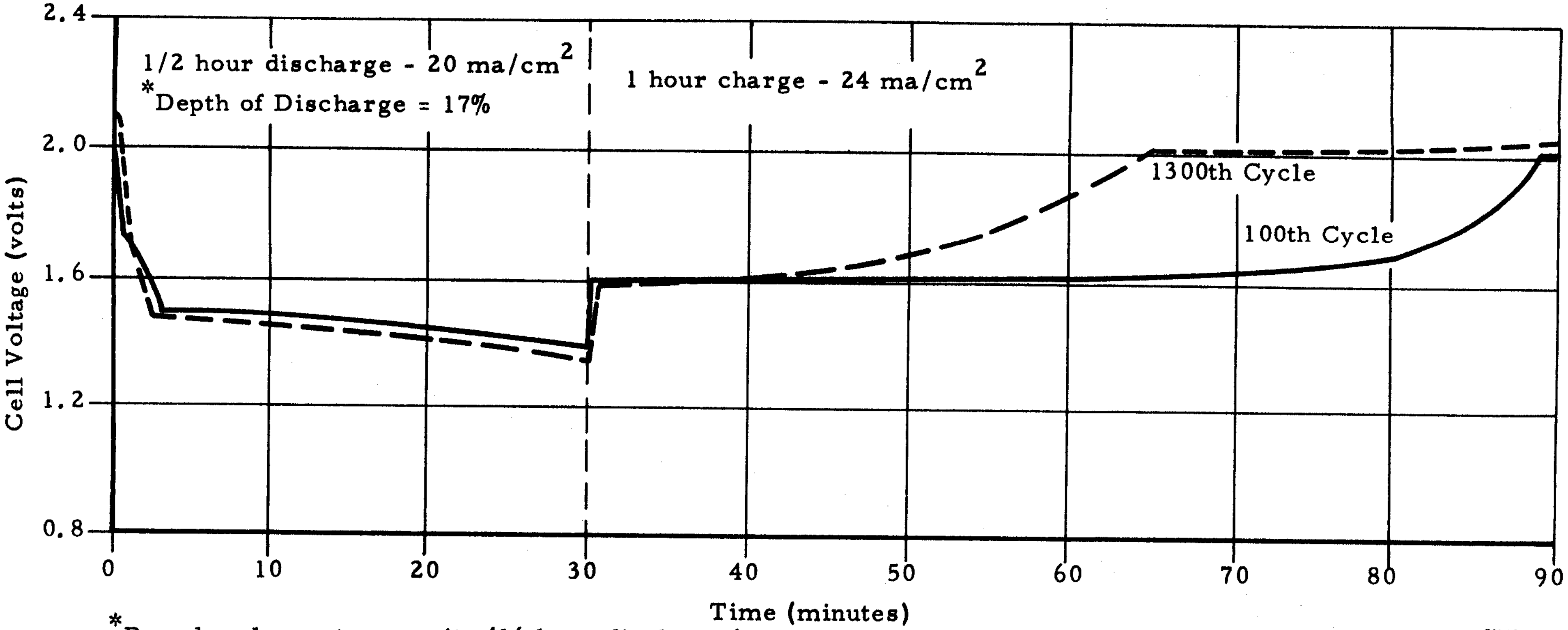

*Based on low rate capacity (16 hour discharge)

Figure 22. Test Cell No. 1873-024 Charge-Discharge Cycle Test Curves at 100° C

TABLE IX

SILVER ZINC CYCLE TEST RESULTS AT 100° C

Cell No.	Silver Electrode	Zinc Electrode	Discharge		Charge		Cycle Temp. °C	Cell Case	Silver Electrode Matrix	Zinc Electrode Matrix	Cycles Compl.
			Time Hrs	I Ma	Time Hrs	I Ma					
1867-040	Paste	Paste	1/2	200	1/2	240	100	Teflon	Ni screen	Ni screen	2286
88-010	Paste	Paste	1/2	200	1	125	100	Teflon	Ni screen	Ni screen	369
88-090	Paste	Paste	1/2	200	1	120	100	Teflon	Ni screen	Ni screen	341
88-080	Paste	Paste	1/2	200	1	120	100	Teflon	Ni screen	Ni screen	190
177-050	Paste	Paste	1/2	200	1	120	100	Teflon	Ni screen	Ni screen	305
177-060	Paste	Paste	1/2	200	1	120	100	Teflon	Ni screen	Ni screen	1072
177-070	Paste	Paste	1/2	200	1	120	100	Teflon	Ni screen	Ni screen	480
177-091	Paste	Paste	1/2	200	1/2	240	100	Teflon	Ni screen	Ni screen	1482
1865-010	Paste	Paste	1/2	200	1	120	100	Teflon	Ni screen	Ni screen	880
1868-033	Paste	Paste	1/2	200	1/2	240	100	Teflon	Ni screen	Ni screen	278
1873-050	Paste	Paste	1/2	200	1/2	240	100	Teflon	Ni screen	Ni screen	288
1893-030	Paste	Paste	1/2	200	1/2	210	100	Teflon	Ni screen	Ni screen	836
1869-040	Paste	Paste	1/2	200	1/2	240	100	Teflon	Ni screen and tab	Ni screen and tab	768
1865-030	Paste	Paste	1/2	200	1	120	100	Teflon	Ni screen	Ni screen	432
1865-040	Paste	Paste	1/2	200	1	120	100	Teflon	Ni screen	Ni screen	1548
1869-020	Paste	Paste	1/2	200	1	120	100	Teflon	Ni screen	Ni screen	794
1873-003	Paste	Paste	1/2	150	1/2	160	100	Teflon	Ni screen and tab	Ni screen and tab	720
1911-050	Paste	Paste	1/2	200	1/2	220	100	Celcon	Ag wire welded to Ni screen	Ag wire welded to Ni screen	1258
1894-010	Paste	Paste	1/2	100	1	60	100	Teflon	Ni screen	Ni screen	1344
1873-024	Paste	Paste	1/2	200	1	120	100	Celcon	Ni screen and Ni wire	Ni screen and Ni wire	1329

TABLE IX (CONT.)

SILVER ZINC CYCLE TEST RESULTS AT 100° C

Cell No.	Silver Electrode	Zinc Electrode	Discharge		Charge		Cycle Temp. °C	Cell Case	Silver Electrode Matrix	Zinc Electrode Matrix	Cycles Compl.
			Time Hrs	I Ma	Time Hrs	I Ma					
152-020	Paste	Paste	1/2	300	1/2	300	100	Celcon	Ni screen	Ni screen	93
152-015	Paste	Paste	1/2	200	1/2	240	100	Teflon	Ni screen	Ni screen	700
128-033	Sintered	Paste	1/2	300	1	180	100	Teflon	Sponge	Ni screen	205
143-010	Sintered	Paste	1/2	300	1	180	100	Teflon	Ni screen	Ni screen	216
152-007	Sintered	Paste	1/2	300	1	180	100	Teflon	Ni screen	Ni screen	576
143-030	Paste	Paste	1/2	300	1	160	100	Teflon	Ni screen	Ni screen	245
143-025	Sintered	Paste	1/2	300	1	160	100	Teflon	Sponge	Ni screen	165
152-060	Sintered	Paste	1/2	300	1/2	360	100	Teflon	Ni screen	Ni screen	232
152-055	Sintered	Paste	1/2	300	1/2	350	100	Teflon	Ni screen	Ni screen	330
152-035	Paste	Paste	1/2	300	1/2	360	100	Teflon	Ni screen	Ni screen	528
143-060	Paste	Paste	1/2	300	1	180	100	Teflon	Ni screen	Ni screen	192
169-035	Ag disc matrix	Paste	1/2	300	1	180	100	Teflon	Ni screen	Ni screen	211
168-090	Paste	Paste	1/2	300	1	180	100	Teflon	Ni screen	Ni screen	92
169-073	Paste	Paste	1/2	300	1	180	100	Teflon	Ni screen	Ni screen	82

cell it was found that the electrodes and the inorganic separator were dry due to the loss of electrolyte. However, the electrodes and separator were in good condition and considerable additional cycle life could have been expected had the test temperature remained as scheduled. Figure 23 is a voltage plot for the first and 97th cycles for this cell. Test Cell No. 152-035 was removed from cycle testing after 528 cycles at 100°C when the Teflon case developed a leak making it impossible to retain electrolyte in the silver electrode compartment. The case had been punctured accidently by the holding clamps used to suspend the test cell in the temperature controlled sand bath. Examination of the cell after disassembly indicated that both electrodes were in good condition, and it was apparent that this cell could have continued for many additional cycles if the case had not been damaged. The method of holding the test cells in the sand baths was changed to prevent a repetition of this problem. As reported previously, the sand baths were subsequently removed from service and replaced with temperature controlled ovens.

Figures 24,25,26,27,28,29, and 30 show typical charge-discharge cycle test curves at 100°C for Test Cell Nos. 177-070, 88-080, 1869-020, 1893-030, 88-090, 168-090, and 1865-010.

In summary, silver-zinc test cells fabricated with Astroset Type 5-036-011 inorganic separators and novel electrodes were cycled at 100°C on a 1/2 hour discharge-one hour charge test schedule at a 17% depth of discharge for as many as 2,286 cycles. Excluding accidental losses and tests terminated for other than electrode or separator reasons, deterioration of the zinc electrode after prolonged cycling was the major reason for termination of the cycle tests at 100°C. These results indicate that although silver-zinc cycle life of 1500 or more cycles at 100°C can be achieved, longer cycle life will be dependent upon further development of the zinc electrode.

3.2.2.2 Cycle Testing at 25°C

In order to provide a basis for comparison of cycle test results at 100°C and for correlation with conventional silver-zinc cells which cannot be tested at elevated temperatures, cycle tests were also made at 25°C during this investigation. These results are given in Table X, which shows the number of cycles obtained and the test conditions.

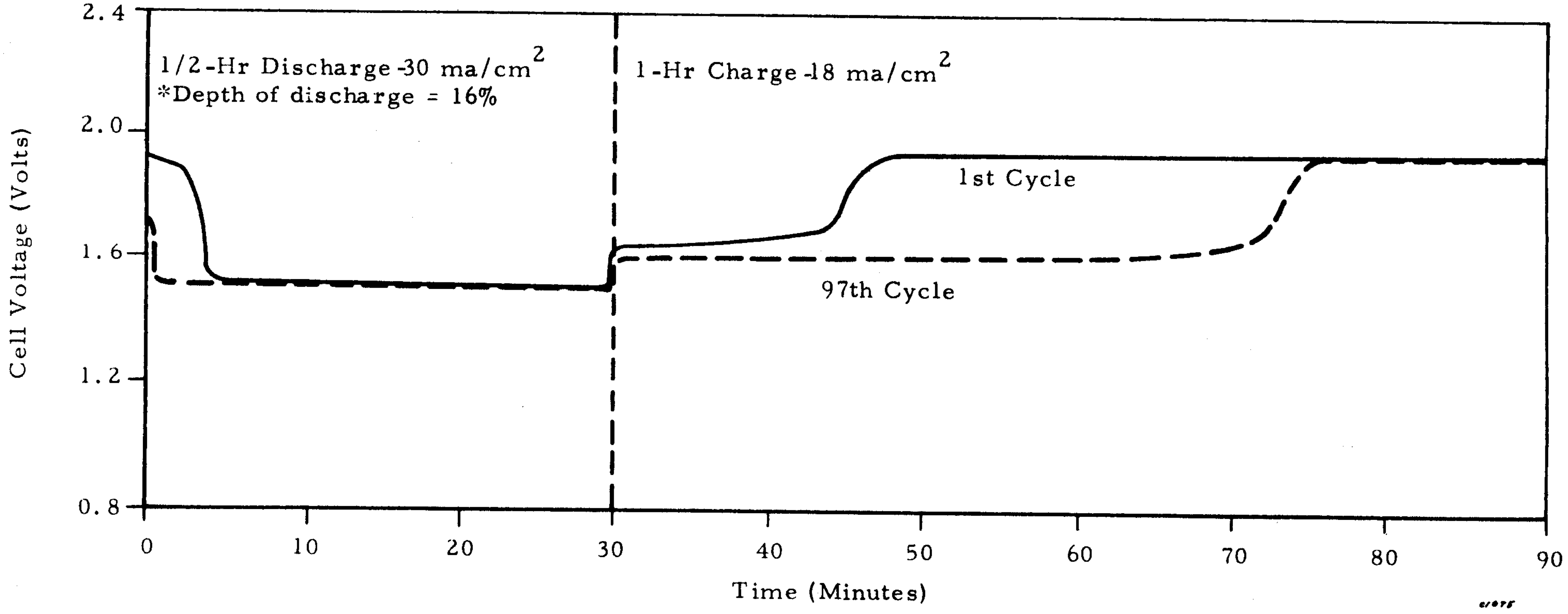

*Based on low rate capacity (16 hour discharge)

Figure 23. Test Cell No. 169-035 Charge Discharge Cycle Test Curves at 100° C

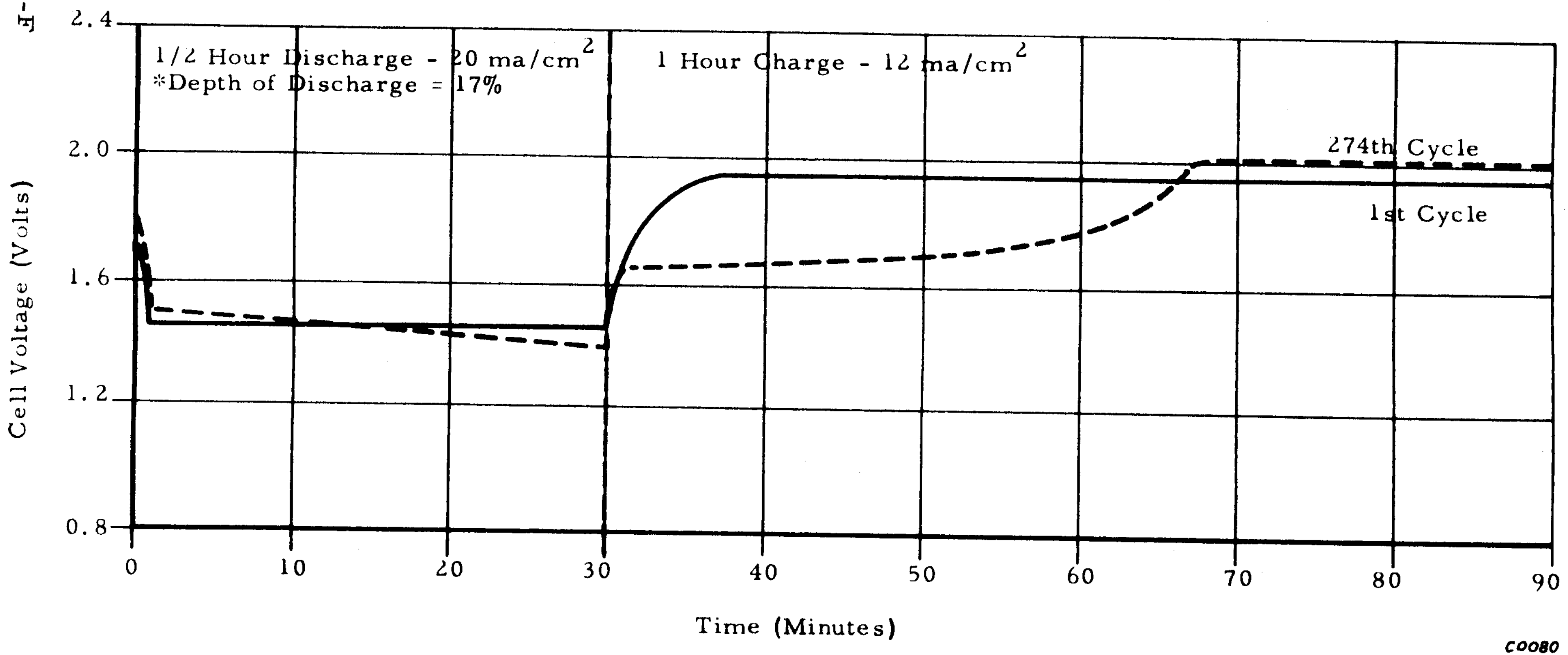

*Based on low rate capacity (16 hour discharge)

Figure 24. Test Cell No. 177-070 Charge-Discharge Cycle Test Curves at 100° C

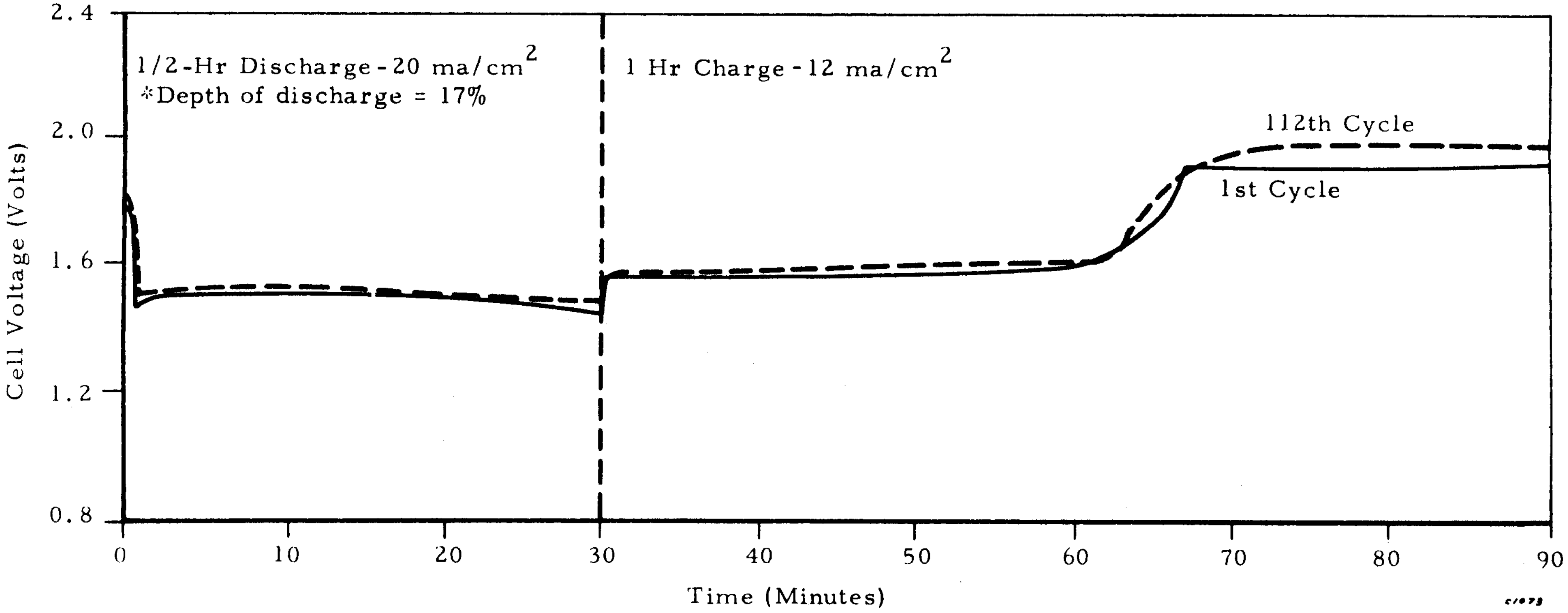

*Based on low rate capacity (16 hour discharge)

Figure 25. Test Cell No. 88-080 Charge-Discharge Cycle Test Curves at 100° C

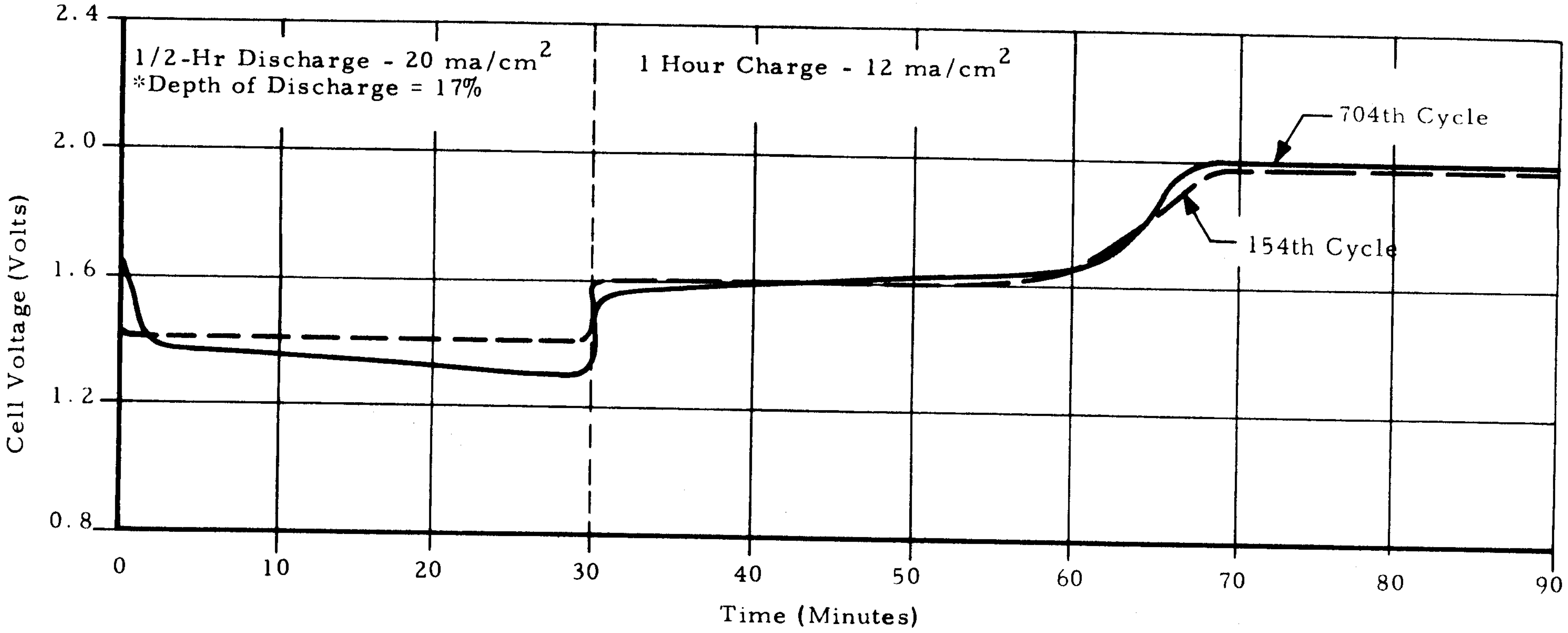

*Based on low rate capacity (16 hr discharge)

Figure 26. Test Cell No. 1869-020 Charge-Discharge Cycle Test Curves at 100° C

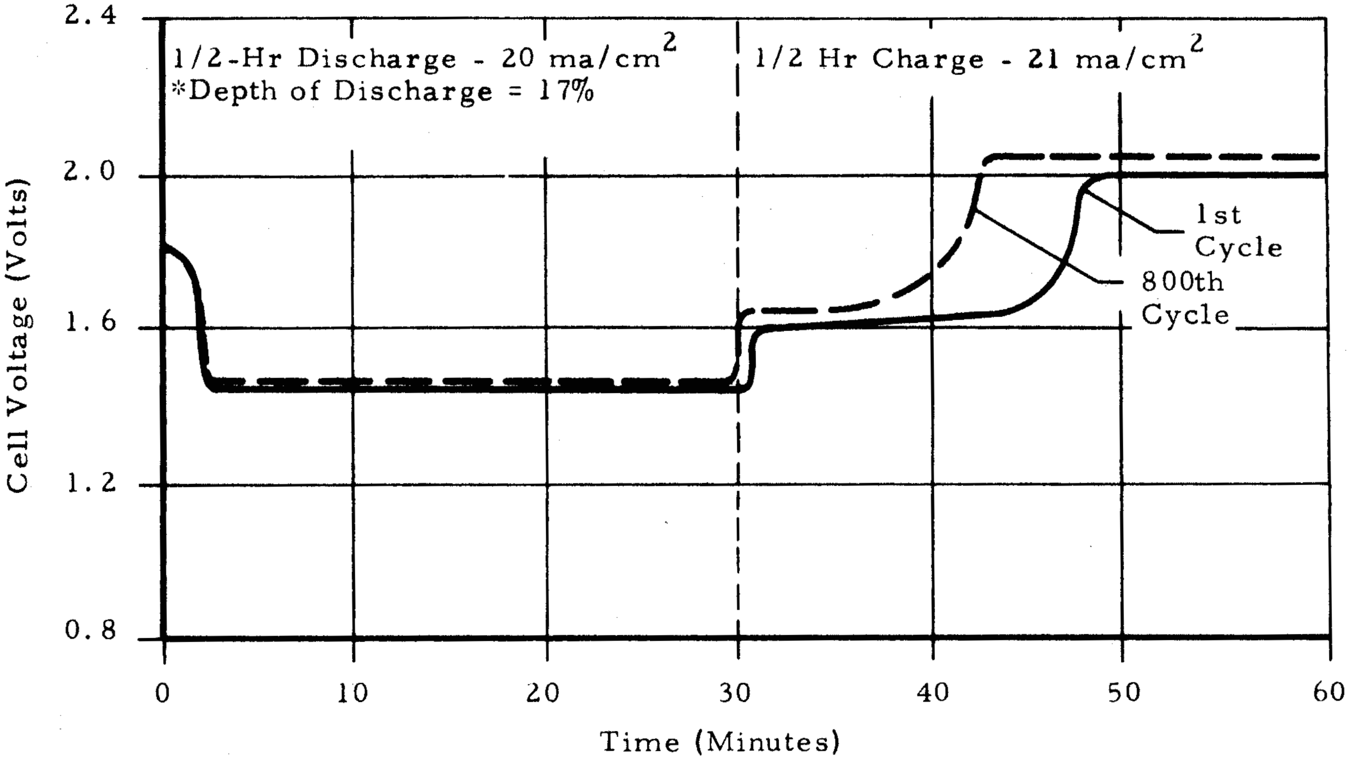

*Based on low rate capacity (16 hr discharge)

Figure 27. Test Cell No. 1893-030 Charge-Discharge Cycle Test Curves at 100° C

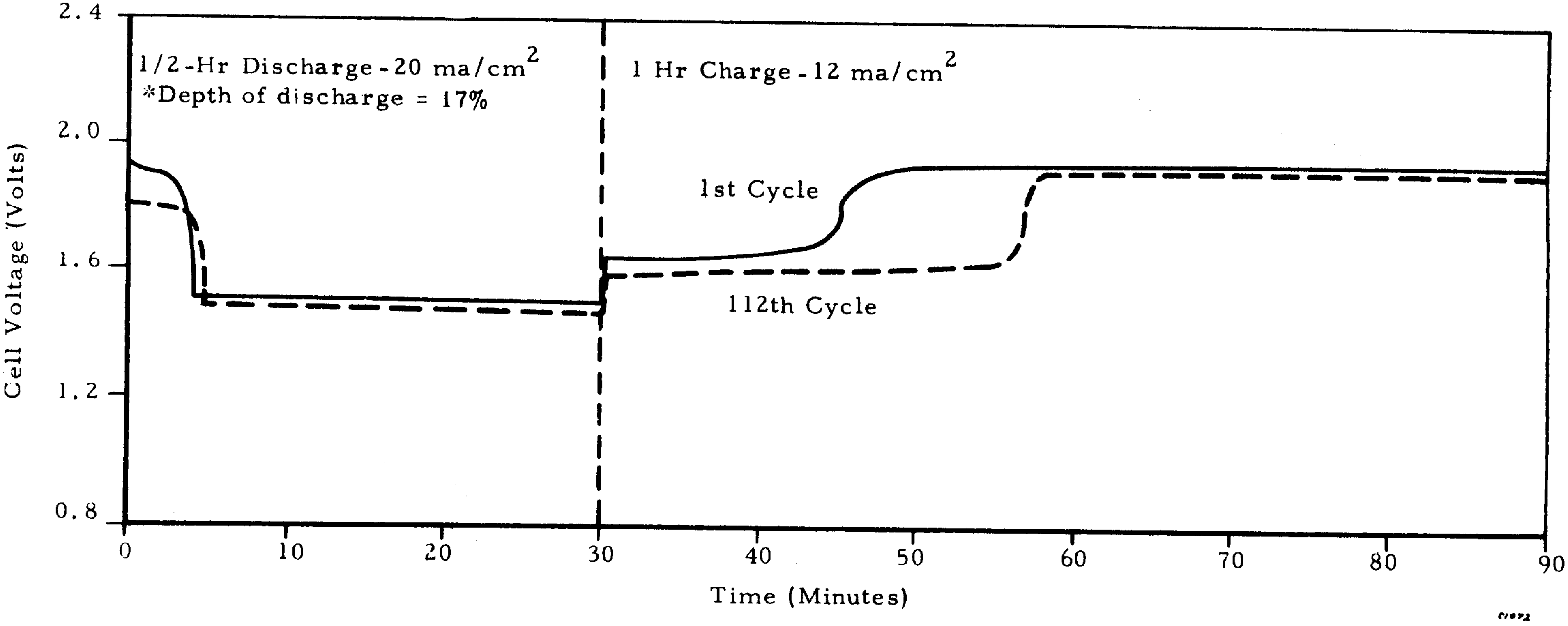

*Based on low rate capacity (16 hour discharge)

Figure 28. Test Cell No. 88-090 Charge-Discharge Cycle Test Curves at 100° C

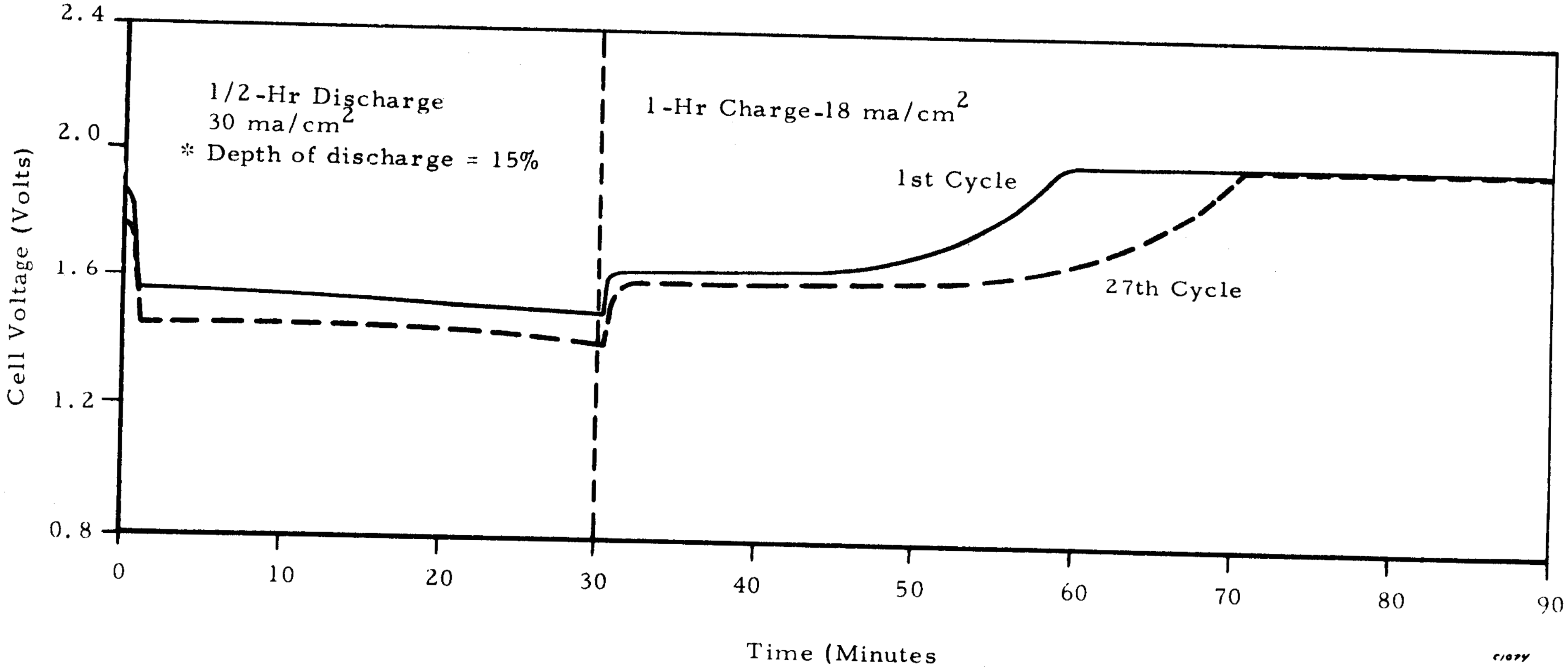

* Based on low rate capacity (16 hr. discharge)

Figure 29. Test Cell No. 168-090 Charge-Discharge Cycle Test Curves at 100° C

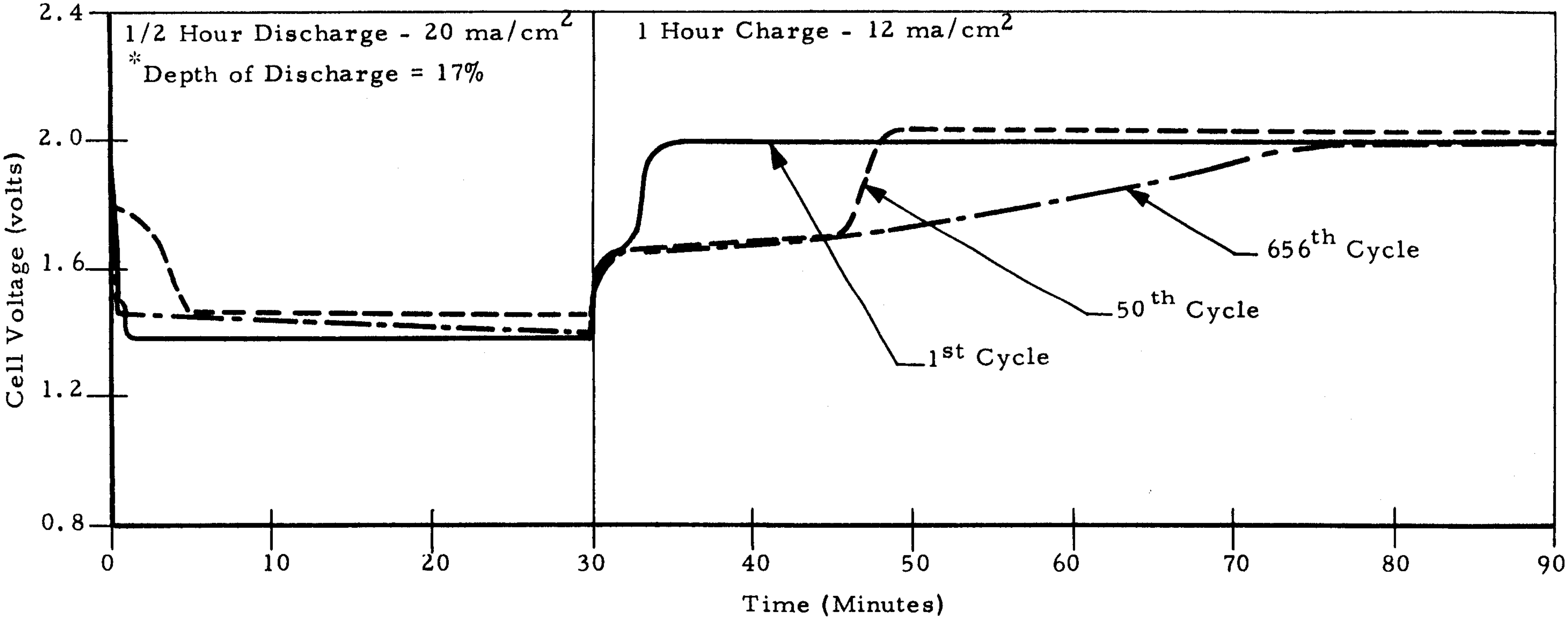

*Based on low rate capacity (17 hour discharge)

Figure 30. Test Cell No. 1865-010 Charge-Discharge Cycle Test Curves at 100° C

TABLE X

CYCLE TEST RESULTS AT 25° C

Cell No.	Silver Electrode	Zinc Electrode	Discharge Time (hrs)	Discharge I (ma)	Charge Time (hrs)	Charge I (ma)	Cycle Temp °C	Cell Case	Silver Electrode Matrix	Zinc Electrode Matrix	Cycles Completed
177-030	Paste	Paste	1/2	200	1	120	25	Teflon	Ni screen	Ni screen	2704
1875-010	Paste	Paste	1/2	85	1	60	25	Teflon	Ni screen	Ni screen	2228
128-062	Sintered	Paste	1/2	300	1	180	100	Teflon	Ni screen	Ni screen	1022
88-095	Paste	Paste	1/2	200	1	120	25	Teflon	Ni screen	Ni screen	2116
177-080	Paste	Paste	1/2	200	1	120	25	Teflon	Ni screen	Ni screen	1228
168-055	Paste	Paste	1/2	200	1	120	25	Teflon	Ni screen	Ni screen	912

Test Cell No. 177-030 satisfactorily completed 2704 cycles at 25°C on a 1/2 hour-1 hour discharge-charge cycle test. Discharge current density was 20 ma/cm^2 and a 17% overcharge was used. Examination of the cell after cycling showed the silver electrode and separator to be in good condition. The zinc electrode was about 70% depleted causing the loss of capacity which resulted in termination of the test. There was also evidence of slight leakage around the separator edges, which could also have contributed to decreased capacity after prolonged cycling. Figure 31 shows typical cycle data for this cell for the first cycle after formation and along with a number of subsequent cycles such as the 976th, 2,350th, and 2,600th cycle.

Figure 32 shows typical cycle performance curves for Test Cell No. 1875-10, which completed 2,228 cycles at 25°C. Test conditions were the same as used for Cell No. 177-030. When disassembled, it was found that the loss of capacity observed after prolonged cycling was due to a 70% depletion of the zinc electrode. The silver electrode was in good condition, but the silver lead wire had corroded, resulting in a high resistance contact. The separator was pinholed in this area of high current concentration.

Test Cell No. 88-095 was removed from 25°C cycle testing after completing 2,116 cycles on the same test schedule used for Nos. 1875-010 and 177-030 due to capacity loss after prolonged cycling. Figure 33 shows typical cycle test performance for the first and 2,133nd cycles, along with several intermediate test cycles. Examination of the cell after disassembly revealed that loss of capacity was due to an 80% depletion of the zinc electrode. As a result of the high current density concentrating in the small remaining electrode area, separator pinholing had also taken place in this area. A chemical analysis of the contents of the electrode compartments showed that there had been leakage of zinc electrode material into the silver compartment as a result.

Other test cells shown in Table X were removed from 25°C cycle testing for various reasons other than separator or electrode deterioration. These reasons for discontinuing the cycle tests included broken contact wires, test equipment malfunction, and case leakage.

In summary, silver-zinc test cells developed during this program using Astroset Type 5-036-011 inorganic separators were

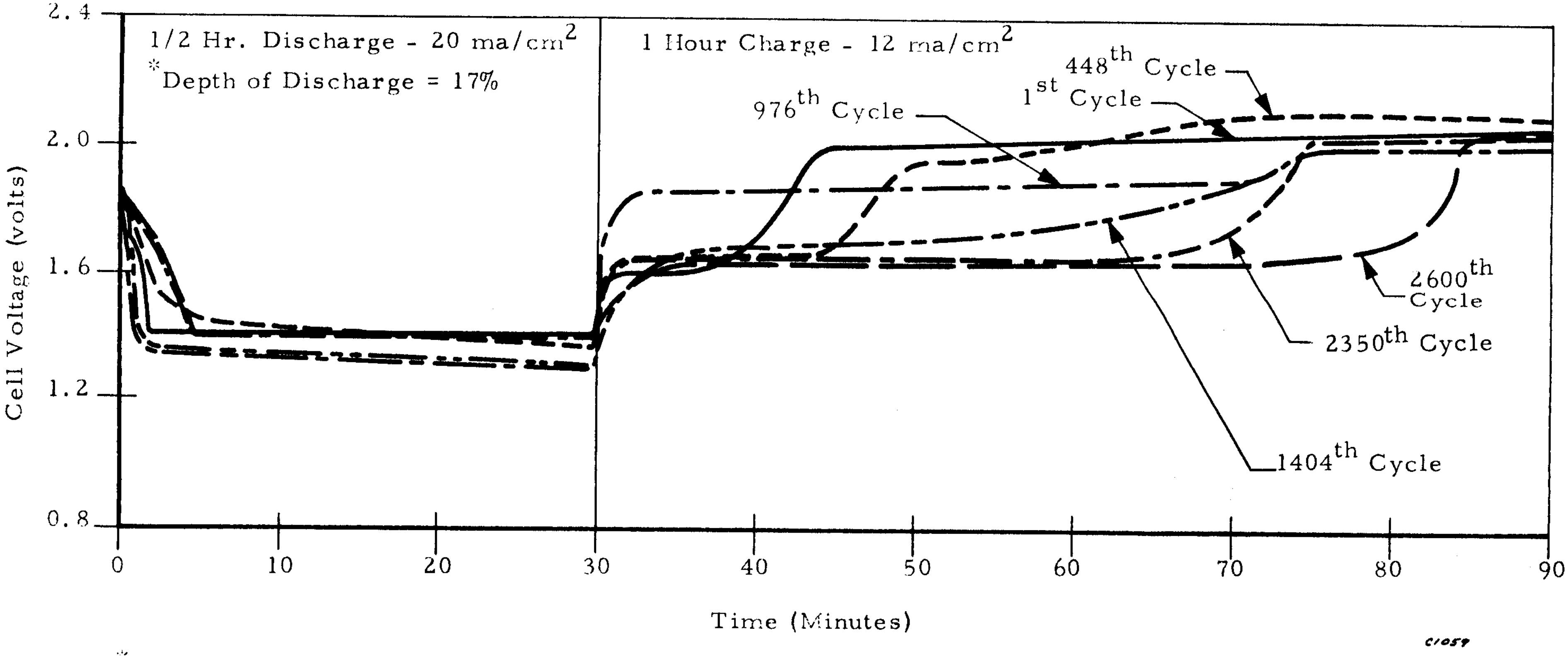

*Based on low rate capacity (16 hour discharge)

Figure 31. Test Cell No. 177-030 Charge-Discharge Cycle Test Curves at 25°C

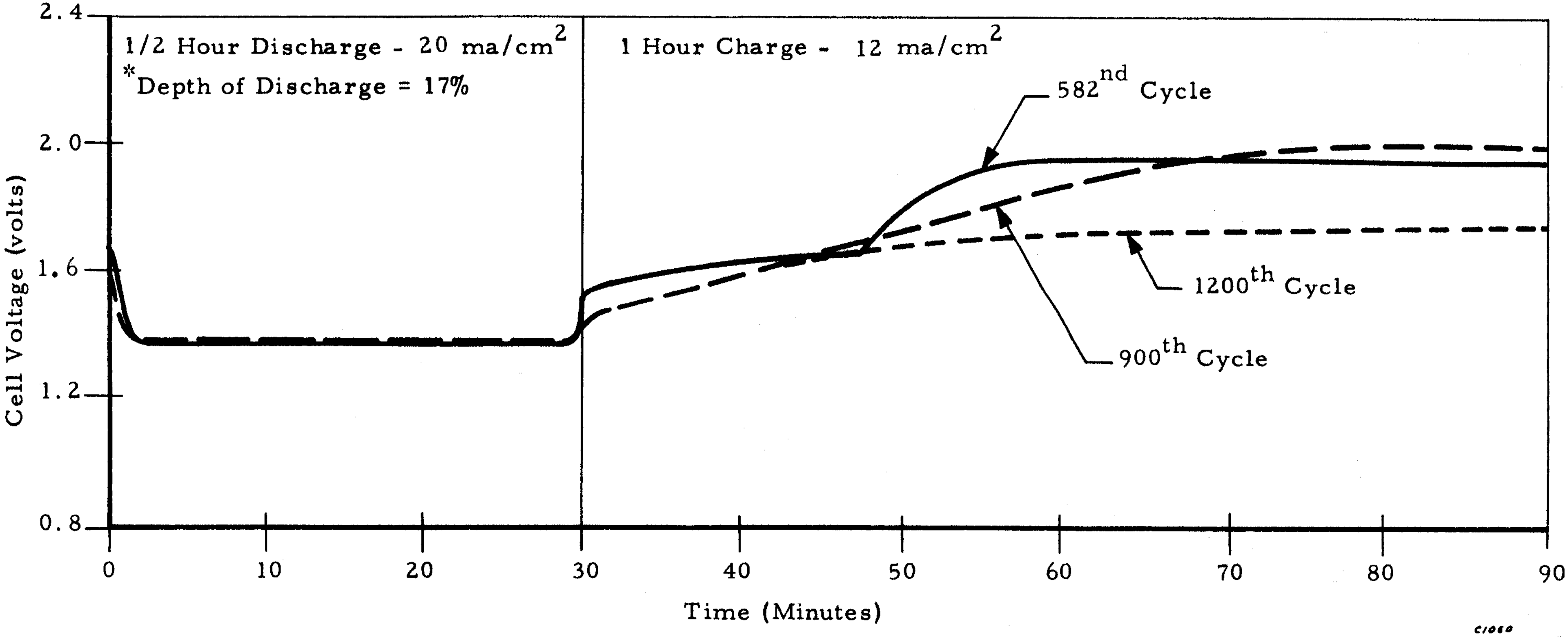

*Based on low rate capacity (16 hour discharge)

Figure 32. Test Cell No. 1875-010 Charge-Discharge Cycle Test Curves at 25°C

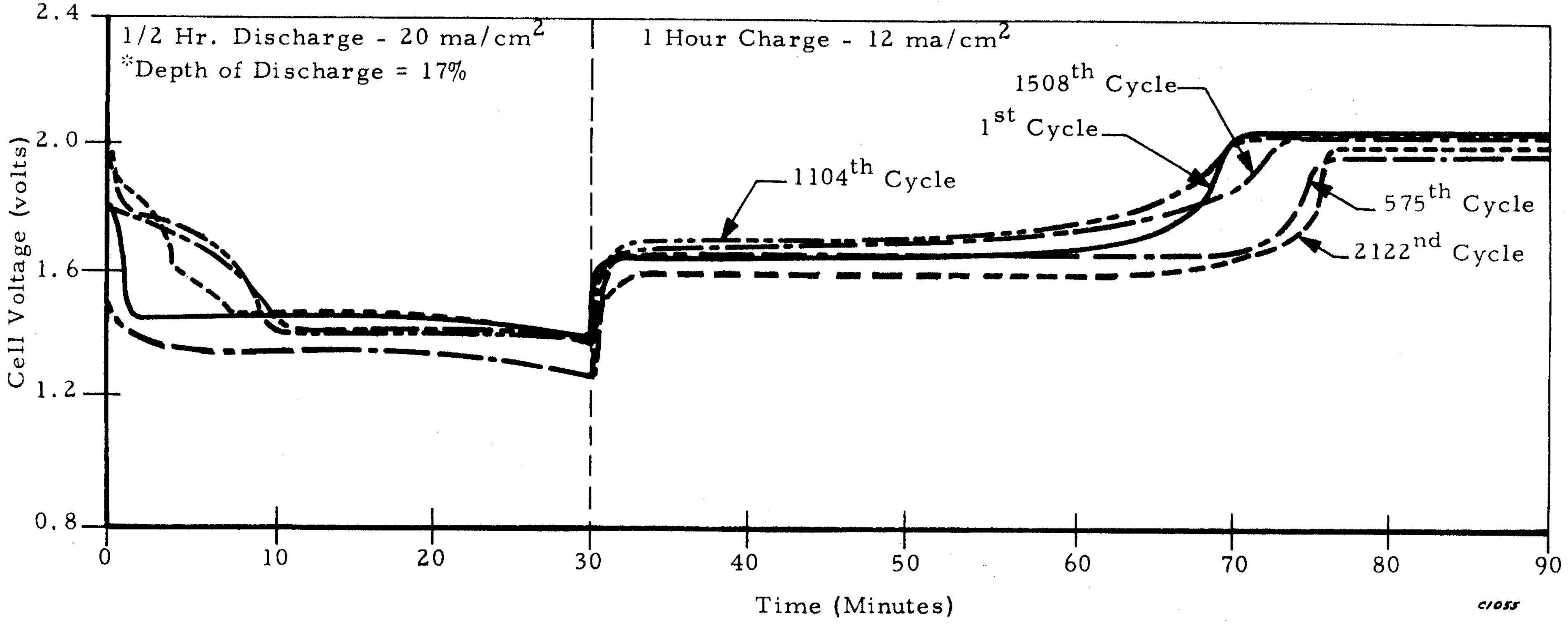

*Based on low rate capacity (16 hr. discharge)

Figure 33. Test Cell No. 88-095 Charge-Discharge Cycle Test Curves at 25° C

discharge. After 11 cycles, loss of capacity developed due to water boil-off caused by the high test temperature. The cell was cycled only during the day shift when water could be added and was permitted to cool to room temperature overnight. After a reduction in capacity during the second day of cycling, the cell was removed from test and fully charged at room temperature. This was followed by a room temperature discharge at 10 ma/cm^2. The cell had a capacity of 0.25 AH, approximately 50% of its initial capacity. After recharging, the test cell was placed on cycle at room temperature on a 1/2 hour discharge (10 ma/cm^2 current density) and a one-hour charge (5 ma/cm^2 current density) schedule to obtain additional experimental cycle data. The test cell successfully completed 2,228 cycles at 25°C when the test was terminated due to further loss of capacity. Upon disassembly, the silver electrode appeared to be normal, while the volume of the zinc electrode was about 75% depleted.

Test Cell No. 1875-20 was fabricated in an identical manner to Test Cell No. 1875-10 and formed to rated capacity. It was then placed on cycle at 150°C on the same test schedule as used for Test Cell No. 1875-10, and at 25% depth of discharge. This cell completed 7 cycles over a two day period prior to a decline in capacity. Following a room temperature charge, the cell delivered approximately 65% of its initial capacity. For evaluation, the test cell was placed in an oven at 100°C ± 1°C and cycled on a 1/2 hour discharge (10 ma/cm^2 current density) and a one hour charge (5.5 ma/cm^2 current density) schedule. After successfully completing 152 cycles, the test cell lost capacity and the test was discontinued. Loss of cell capacity was attributed to partial depletion of the zinc electrode.

It can be concluded from these tests at 125°C and 150°C that Type 5-036-011 inorganic separators can be cycled for several days at these temperatures. However, depletion of the zinc electrode, which is accelerated by high temperatures, limits cycle life of the test cells to a considerable extent.

3.2.3 Commercial Electrode Evaluation

NASA-Lewis Technical Direction No. 2, dated 21 May 1965, requested Astropower Laboratory to fabricate two standard single test cells using capable of as many as 2,704 discharge-charge cycles on a 1/2 hour discharge-1 hour charge test schedule at 17% depth of discharge. For comparison, typical commercial silver-zinc cells cycled at the same current density and depth of discharge failed after 5 to 10 cycles at 25°C when tested by this laboratory.

3.2.2.3 Test Cell Evaluation at 125°C and 150°C

The work statement for Contract NAS 3-6007 also required Astropower Laboratory to evaluate improved inorganic separators and electrodes, at 125°C and 150°C. Test cells were fabricated in accordance with standard cell design and formed as described in previous sections of this report resulting in a cell capacity after formation of 0.5-0.6 ampere-hour.

Test Cell No. 1875-30 was prepared using standard silver and zinc electrode formulations, a Type 5-036-011 inorganic separator and Teflon cell cases. After formation, the test cell had a capacity of 0.5 ampere-hours. It was then placed in a temperature controlled oven at 125°C ± 1°, and continuously cycled on a 1/2 hour discharge and one hour charge schedule. The test cell was discharged to 25% depth of discharge and was given a 20% overcharge. The discharge current density was 20 ma/cm^2. This test cell was cycled for 83 cycles with normal results. When the electrodes dried out due to the high temperature the test was terminated. After reactivation with distilled water, cycling was continued for an additional 3-1/2 days, water being added as required to keep the electrodes wet.

Examination of the test cell showed that it had developed internal shorting due to leakage of electrolyte around the edge of the inorganic separator but both the electrodes and the separator were in good condition.

Test Cell No. 1875-10 was assembled using standard paste silver and zinc electrodes and a type 5-036-011 inorganic separator. The test cell was formed in the standard manner to 0.5 AH capacity. The cell was then placed in a temperature controlled oven and continuously cycled at 150°C ± 1° on a 1/2 hour charge (36 ma/cm^2 current density) and a 1/2 hour discharge (36 ma/cm^2 current density) test schedule at 25% depth of commercial silver and zinc electrodes and Type 5-036-011 inorganic separators. The purpose of these cycle tests was to establish a baseline against which Astropower Laboratory electrodes might be compared using the Type 5-036-011 inorganic separators.

One test cell was to be cycled at 25°C on a 1/2 hour discharge by one-hour charge cycle. The other cell was to be cycled on the same cycle schedule at 100°C.

Test Cell No. 1929-50 was constructed in a Celcon case using silver and zinc electrode obtained from a commercial 5 ampere-hour secondary cell and a Type 5-036-011 inorganic separator. The active area of the commercial electrodes was approximately 17 cm^2. The cell was formed in 45% KOH in accordance with the procedure specified by the manufacturer of the 5 ampere-hour cell and had 0.825 ampere-hour capacity at low rate.

As NASA Technical Direction No. 2 specified that these test cells were to be discharged at 25°C at a current density of 20 ma/cm^2, the cell was placed on 1/2-hour discharge at 350 ma and one-hour charge at 193 ma. This resulted in 10% overcharge and about 21% depth of discharge. After 366 cycles the cell began to lose capacity and would not accept a full charge. The cycle test was discontinued. (See Figure 34).

Upon disassembly the silver electrode was found to be in good condition although it was warped toward the case. The zinc electrode had slumped badly. It was also noted that the silver current collector used in the zinc electrode had completely eroded leaving only a sharp pointed terminal wire. The inorganic separator was pinholed where it touched the sharp point of the terminal wire. This was caused by the extremely high current density at this point resulting in localized heating which eventually burned a hole through the separator.

Cell No. 3261-01 was assembled in a Celcon case in a similar manner as Test Cell No. 1929-50 using silver and zinc electrodes obtained from a commercial 5 ampere-hour cell from the same manufacturer and a Type 5-036-011 inorganic separator which was 0.021 inch thick.

The capacity of this cell was 0.675 ampere-hour following formation. The cell was placed on cycling at 100°C on a 1/2 hour discharge at

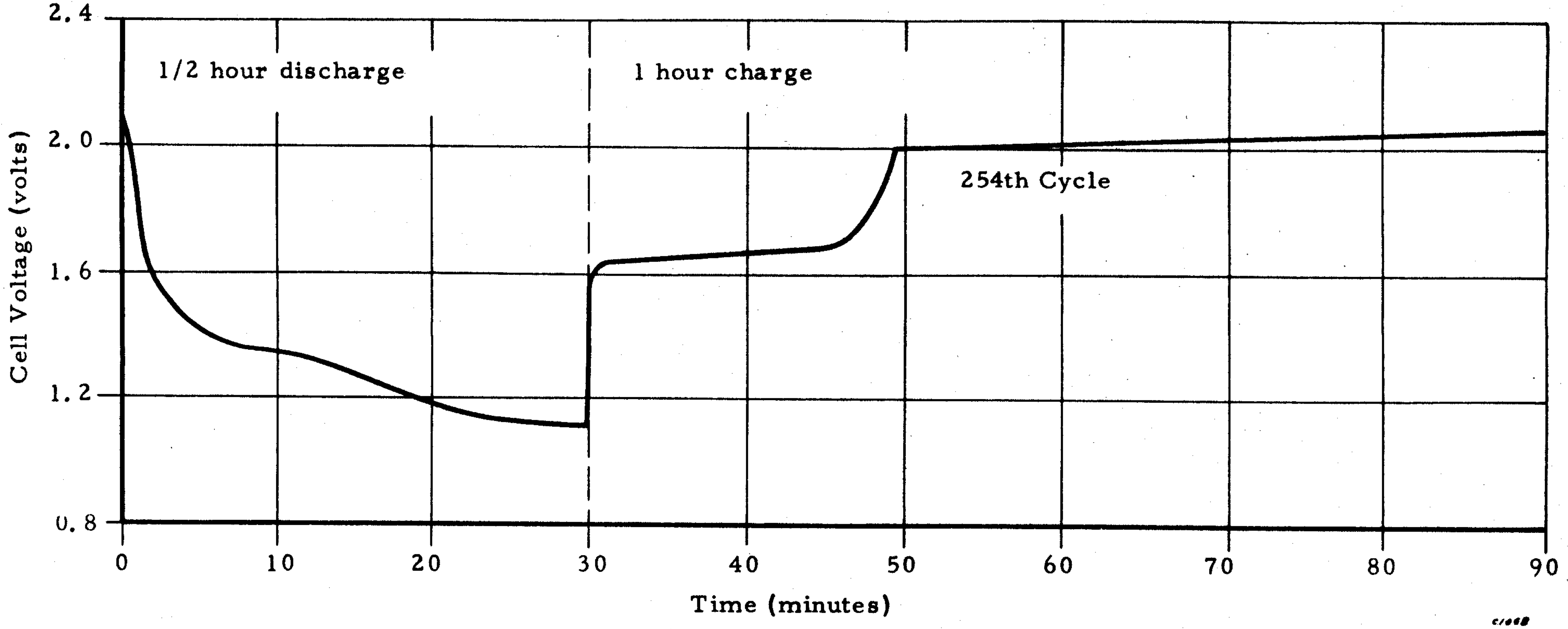

Figure 34. Test Cell No. 1929-50. 100°C Temperature Cycle Curve on Test Cell Containing Commercial Electrodes and Type 5-036-011 Inorganic Separator.

350 ma and a one-hour charge at 193 ma resulting in a discharge current density of 20 ma/cm^2, 10% overcharge, and 26% depth of discharge. The test cell successfully completed a total of 204 cycles at 100°C after which it lost capacity, (See Figure 35). The cell was removed from cycling, charged manually, then discharged manually, and exhibited 22% capacity. The cell was disassembled and it was found that the commercial silver electrode was in good condition although it was warped. The zinc electrode had slumped approximately 75% within the cavity and the silver current collector wire had eroded into two pieces. The inorganic separator was in good condition.

It can be generally concluded from these tests that commercially made silver and zinc electrodes are capable of several hundred cycles in the temperature range 25° - 100°C when assembled with Type 5-036-011 inorganic separators. Greater cycle life at both 100°C and 25°C can be attained, however, using the silver and zinc electrode formulations developed by Astropower Laboratory and Type 5-036-011 inorganic separators. These experimental test cells cycle many hundreds of times at either temperature before deterioration or failure.

As discussed above, this longer cycle life is due in part to the superior current collector-terminal connector design used in the Astropower test cells which avoids erosion and excessive current density concentration.

3.2.4 Comparison of Gassing Characteristics of Astropower Laboratory and Commercial Silver and Zinc Electrodes at 25°and 100°C

An important characteristic of electrodes used in batteries is their gassing performance. Gas evolution during charge-discharge cycling represents not only inefficiency but also presents the problem of designing battery cases strong enough to withstand the pressures developed in sealed battery systems.

The gassing characteristics of Astropower Laboratory silver-zinc paste electrodes were determined under charge-discharge cycling at room temperature and at 100°C and compared to commercial silver-zinc electrodes in order to provide information for sealed cell design considerations.

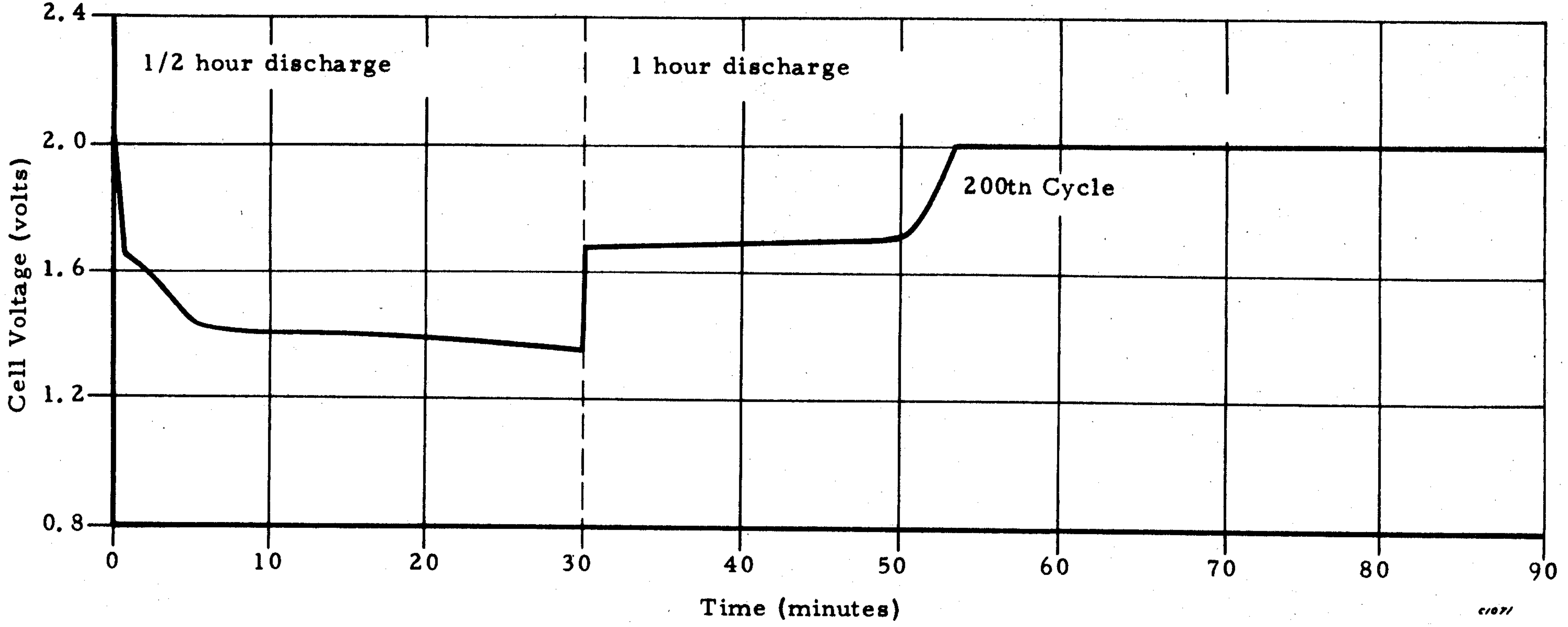

Figure 35. Room Temperature Cycle Curve on Test Cell Containing Commercial Electrodes and Type 5-036-011 Inorganic Separator

Technical Direction No. 2, dated 21 May 1965 requested Astropower Laboratory to measure gas pressures developed during cycling, under the following conditions:

(a) Standard Astropower Laboratory cell cycled at 25°C

(b) Standard Astropower Laboratory cell cycled at 100°C

(c) Cell assembled with silver and zinc electrodes from a commercial battery with Type 5-036-011 inorganic separator cycled at 25°C.

(d) Cell assembled with silver and zinc electrodes from a commercial battery with Type 5-036-011 inorganic separator cycled at 100°C.

The test cells were cycled on a 1/2 hour discharge (20 ma/cm^2 current density) and one hour charge (12 ma/cm^2 current density) test schedule.

3.2.4.1 Test Apparatus

The silver-zinc electrode system was evaluated in a standard Ag-Zn test cell, using Type 5-036-011 inorganic separators to isolate the electrode compartments. As a means of confining the gases developed during charge-discharge cycling, the test cell was contained in a closed stainless steel cylinder. A photograph of the test apparatus is shown in Figure 36. The top of the pressure vessel was provided with ceramic terminals for electrical connections, inlet and outlet gas valves, and pressure gauge to measure the total pressure of the gases formed during cycling. A temperature controlled oven was used for the 100°C tests.

3.2.4.2 Test Procedure

The silver-zinc test cell was placed in the steel cylinder which was then filled with glass balls to minimize the volume of void space. The sealed cylinder was then tested using nitrogen at 30 lbs/in^2. The void space within the steel cylinder was determined by the expansion of a given mass of gas into an evacuated glass blub of known volume. In this procedure, the initial and final pressure are measured and the ideal gas law was used to calculate the volume of the steel cylinder. Prior to cycling, the cylinder

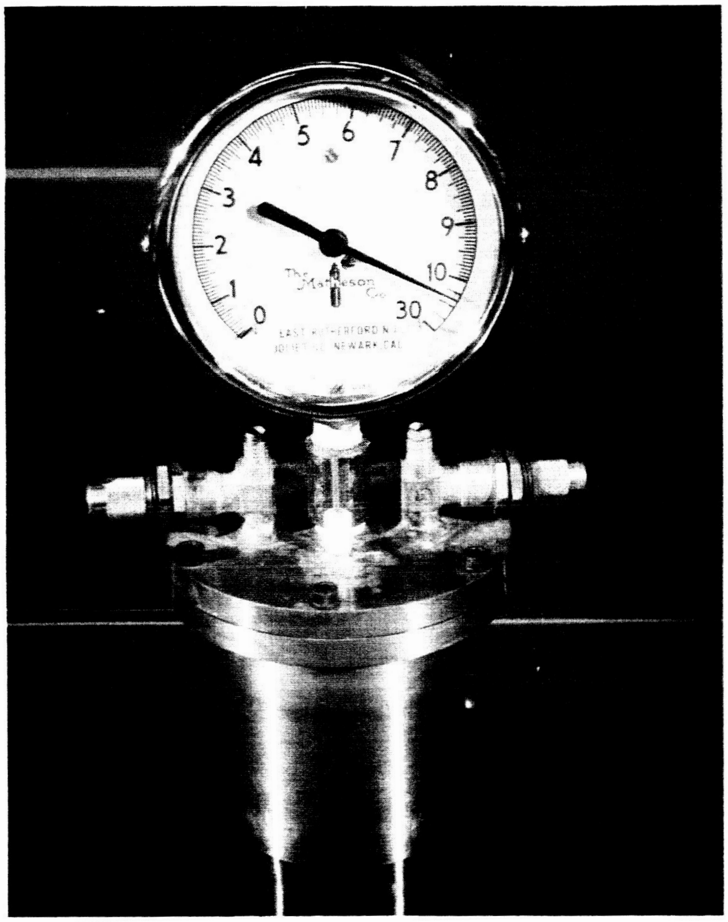

Figure 36. Gassing Test Fixture

was swept with nitrogen to exclude air, and then filled with nitrogen gas and pressurized at 2.0 lbs/in^2 to provide a uniform starting point for the gassing experiments. The test cell was subjected to discharge-charge cycling and the total pressure of the gaseous mixture was measured as a function of time during continuous cycling.

Prior to determination of the gassing characteristics of test cells, they were subjected to two discharges (100% depth) in order to form the electrodes. After the second discharge, the test cells were charged and placed into the sealed container for gassing tests.

Test cells were cycled on a 1/2-hour discharge-one hour charge cycle at constant current.

At room temperature, the Astropower Laboratory experimental cell was discharged at 200 ma (1/2 hour) followed by a charge of 120 ma (1 hour). The discharge rate corresponds to a current density of 20 ma/cm^2 and 20% depth of discharge based upon a nominal 0.5 ampere-hour capacity.

The same current density was used for the cell containing the commercial electrodes. Both cells were giving a 20% overcharge during cycling.

For the gassing measurements at 100°C, both cells were cycled at the same current, (200 ma discharge (1/2 hour) and 120 ma charge (1 hour)). Consequently, the current density of the commercial electrodes was 13 ma/cm^2 compared to 20 ma/cm^2 for Astropower Laboratory electrodes. Finally, the same overcharge, (20%) was used for both of the electrode systems in order to obtain substantial gassing rates.

3.2.4.3 Electrode Gassing Characteristics at Room Temperature

A comparison of the gassing behavior of Astropower Laboratory silver-zinc electrodes with the silver-zinc electrodes obtained from a commercial silver-zinc battery is shown in Figure 37 and summarized in Tables XI and XII. During 90 hours of cycling (60 cycles), the Astropower Laboratory electrodes exhibited substantially less gassing than the commercial electrodes. Comparison of the pressures developed after

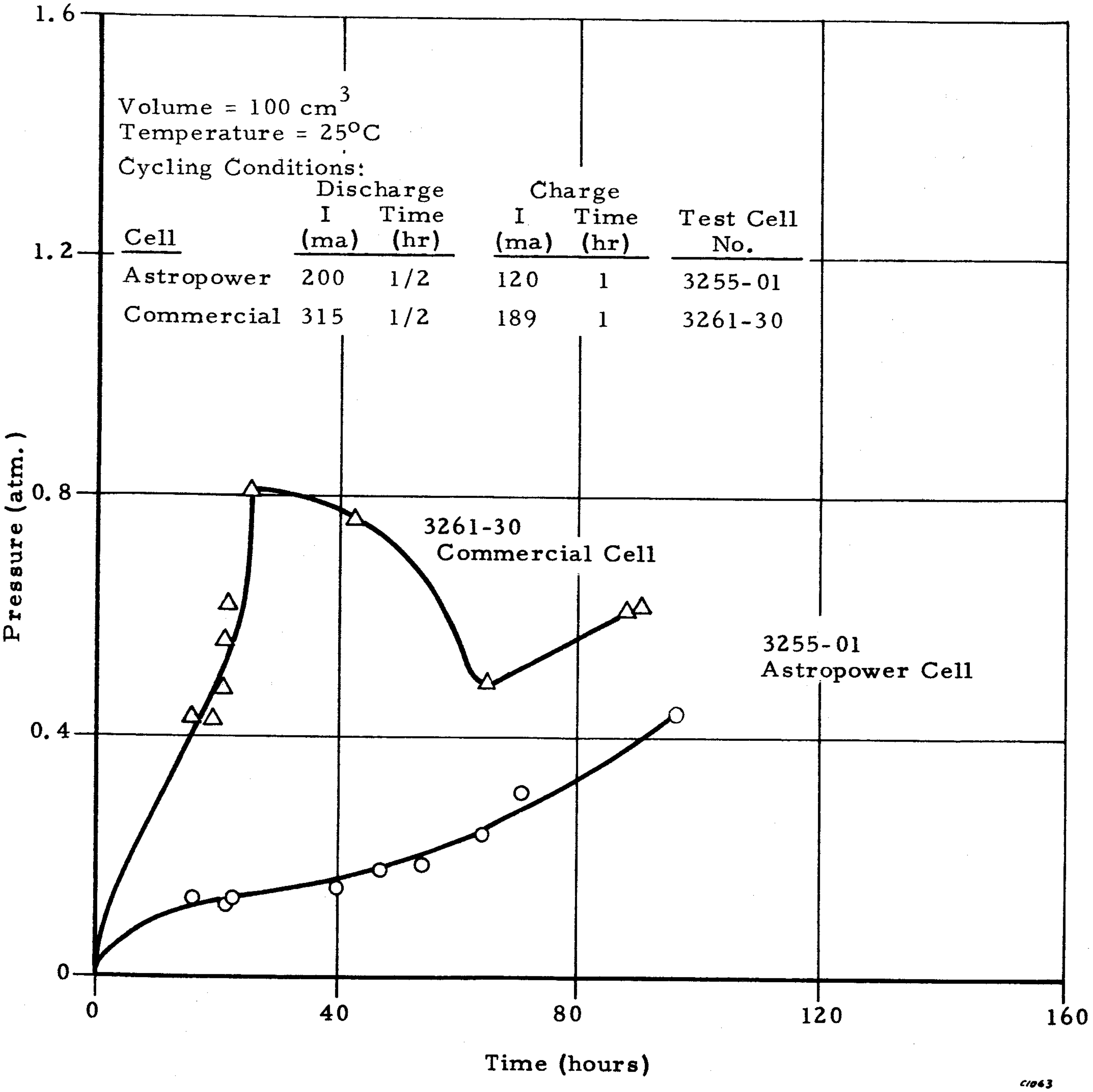

Volume = 100 cm^3
Temperature = 25°C
Cycling Conditions:

Cell	Discharge I (ma)	Discharge Time (hr)	Charge I (ma)	Charge Time (hr)	Test Cell No.
Astropower	200	1/2	120	1	3255-01
Commercial	315	1/2	189	1	3261-30

Figure 37. Comparison of Gassing during Cycling of Astropower Electrodes with Commercial Electrodes

TABLE XI

GASSING CHARACTERISTICS OF TEST CELL NO. 3255-01 AT ROOM TEMPERATURE

Cycling Conditions: 1/2 hr discharge, 1 hr charge
(200, 120)

Time (hr)	No. of Cycles	Pressure (V = 100 cm^3) lbs/in^2	Pressure (V = 100 cm^3) atm.	t 25°C
0	0	0	0	
16.2	10.8	1.88	0.13	
21.7	14.5	1.81	0.12	
22.7	15.2	1.88	0.13	
40.2	26.8	2.17	0.15	
42.7	28.5	2.34	0.16	
47.2	31.5	2.60	0.18	
54.4	36.3	2.80	0.19	
64.2	42.8	3.47	0.24	
70.8	47.2	4.51	0.31	
112.9	75.3	9.40	0.64	

TABLE XII

GASSING CHARACTERISTICS OF TEST CELL NO. 3261-30 at 25° C

Cycling Conditions: 1/2 hr discharge, 1 hr charge
(315, 189) ma

Time (hr)	No. of Cycles	Pressure (V = 100 cm^3) lbs/in^2	Pressure (V = 100 cm^3 atm.	t 25° C
0	0	0	0	
15.7	10.5	6.26	0.43	
19.5	13.0	6.26	0.43	
20.7	13.8	7.04	0.48	
21.1	14.0	8.18	0.56	
21.4	14.2	9.13	0.62	
21.7	14.5	9.13	0.62	
22.4	15.0	9.13	0.62	
25.7	17.2	11.9	0.81	
26.1	17.4	11.6	0.79	
26.7	17.8	11.1	0.76	
43.1	28.7	11.1	0.76	
64.6	43.0	7.15	0.49	
88.1	58.7	9.00	0.61	
89.9	60.0	9.13	0.62	

20 hours of cycling shows that the commercial electrodes developed almost four times as much gas as Astropower Laboratory electrodes resulting in a pressure of 0.49 atm. compared to 0.13 atmospheres (in a volume of 100 cm^3). After cycling for 90 hours, the commercial electrodes were gassing more than 1.6 times as much as the experimental electrodes. The improved gassing performance of Astropower electrode configurations is evidently related to formulation, especially in the case of zinc electrode where the mercuric oxide content is important, as well as physical design. Further study of the gassing characteristics of Astropower electrodes should be made in view of the importance of improved gassing performance in sealed batteries especially for applications which require thermal sterilization. This work can also result in the development of an understanding of the mechanism involved which will also permit further improvement.

Examination of the upper curve in Figure 37 indicates complex dependance of pressure with time with the commercial silver-zinc electrodes. This curve has three branches; (a) a sharp rise in pressure terminating in maximum pressure after 26 hours of cycling. (b) a sharp decrease in pressure during cycling in the time interval from 26 to 65 hours, caused by chemical or electrochemical reactions of the gas mixture with the electrodes, and (c) a marked rise in pressure in the time interval from 65 to 90 hours during cycling.

On the other hand, the curve showing the gassing of Astropower Laboratory electrodes exhibits a low rate of gassing during the first 26 hours of cycling (0.13 atm.).

3.2.4.4 Gassing at 100°C

Comparison of the gassing rates at 100°C as a function of time for Astropower Laboratory electrodes with commercial electrodes is shown in Figure 38 and summarized in Tables XIII and XIV. The upper curve in Figure 38 represents the commercial electrodes and has the same shape as that for the Astropower Laboratory electrodes. In both cases, a rapid rate of gassing takes place during the first three hours of cycling (2 cycles) with a pressure of 1.02 atm. ($v = 121/cm^3$ for the Astropower Laboratory electrodes and a higher pressure of 1.6 atm ($v = 154\ cm^3$) for the

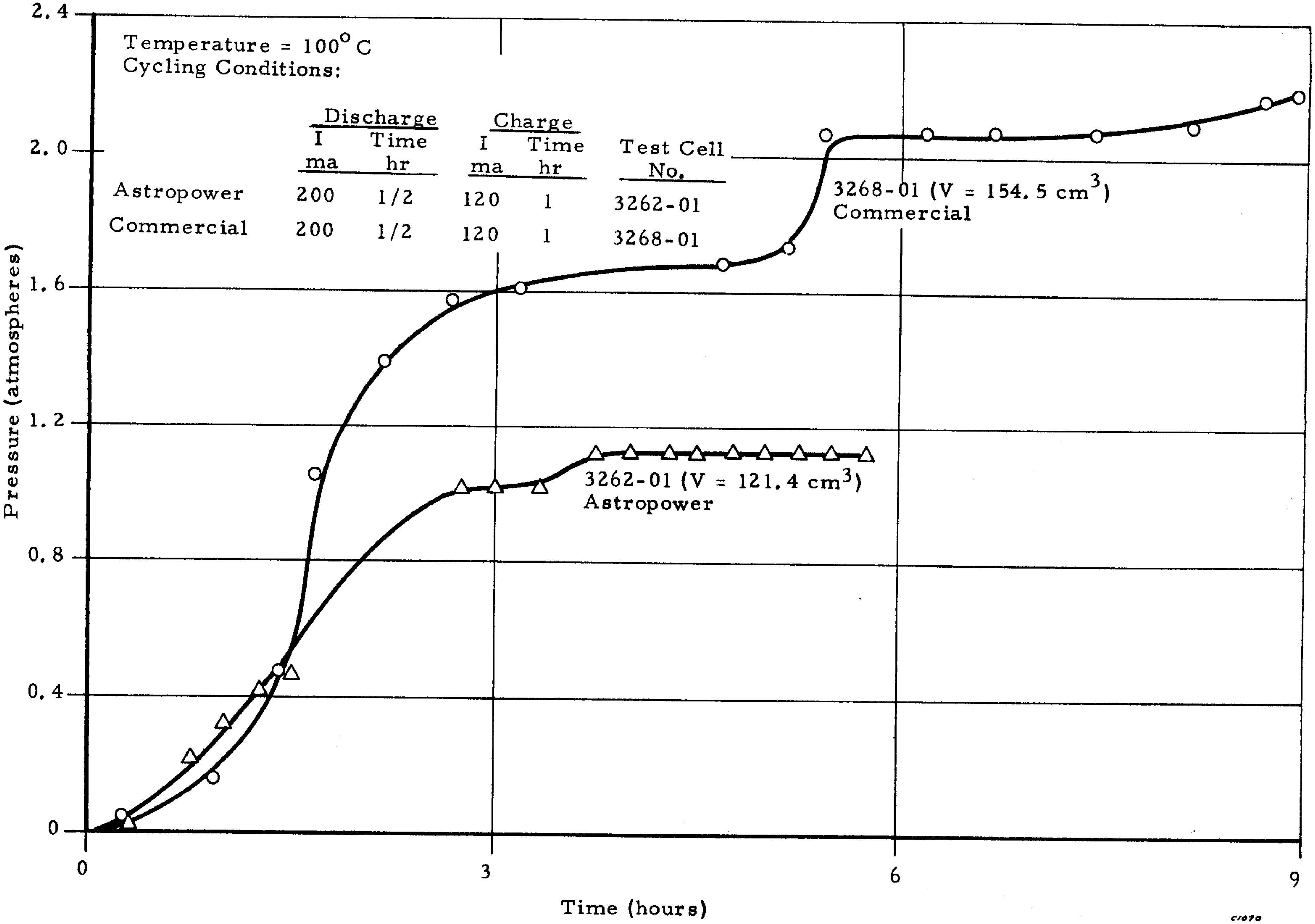

Figure 38. Comparison of Gassing during Cycling of Astropower Electrodes with Commerical Electrodes

TABLE XIII

GASSING CHARACTERISTICS OF TEST CELL NO. 3268-01 AT 100° C

Cycling Conditions: 1/2 hr discharge, 1 hr charge
(200, 120) ma

Time (hr)	No. of Cycles	Pressure of Wet Gas ($V = 154.5\ cm^3$) lbs/in^2	Pressure of Wet Gas ($V = 154.5\ cm^3$) atm.	t 100°C
0	0	-0.5	-0.03	
0.17	0.11	0.25	0.02	
0.25	0.17	0.75	0.05	
0.33	0.22	1.25	0.08	
0.42	0.28	1.50	0.10	
0.67	0.45	2.90	0.20	
0.67	0.45	1.65	0.11	
0.92	0.61	2.40	0.16	
1.17	0.78	4.15	0.28	
1.42	0.95	6.90	0.47	
1.67	1.11	15.40	1.05	
1.92	1.28	17.90	1.22	
2.17	1.45	20.40	1.39	
2.42	1.61	22.40	1.52	
2.67	1.78	23.10	1.57	
2.92	1.95	23.40	1.59	
3.17	2.11	23.65	1.61	
3.42	2.28	23.90	1.63	
3.67	2.45	23.40	1.59	
3.92	2.61	24.65	1.68	
4.17	2.78	24.65	1.68	
4.42	2.95	24.90	1.69	
4.67	3.11	24.90	1.69	
4.92	3.28	25.15	1.71	
5.17	3.45	25.40	1.73	
5.42	3.61	30.40	2.07	
5.67	3.78	30.40	2.07	
6.17	4.11	30.40	2.07	
6.42	4.28	30.40	2.07	
6.67	4.45	30.40	2.07	
6.92	4.61	30.40	2.07	
7.17	4.78	30.40	2.07	
7.42	4.95	30.40	2.07	
7.67	5.11	30.40	2.07	
7.92	5.28	30.40	2.07	
8.17	5.45	30.90	2.10	
8.42	5.61	31.65	2.15	
8.67	5.78	31.90	2.17	
8.92	5.95	32.15	2.19	

TABLE XIV

GASSING CHARACTERISTICS OF TEST CELL NO. 3262-01 AT 100° C

Cycling Conditions: 1/2 hr discharge, 1 hr charge
(200, 120) ma

Time (hr)	No. of Cycles	Pressure of Wet Gas ($V = 121.4 \text{ cm}^2$) lbs/in^2	Pressure of Wet Gas ($V = 121.4 \text{ cm}^2$) atm.	t 100°C
0	0	-0.25	-0.02	
0.25	0.17	0.50	0.03	
0.75	0.50	3.25	0.22	
1.0	0.67	4.75	0.32	
1.25	0.83	6.00	0.41	
1.50	1.00	6.75	0.46	
2.75	1.83	15.0	1.02	
3.00	2.00	15.0	1.02	
3.33	2.22	15.0	1.02	
3.75	2.50	16.5	1.12	
4.00	2.67	16.5	1.12	
4.25	2.83	16.5	1.12	
4.50	3.00	16.5	1.12	
4.75	3.17	16.5	1.12	
5.00	3.33	16.5	1.12	
5.25	3.50	16.5	1.12	
5.50	3.67	16.5	1.12	
5.75	3.83	16.5	1.12	

commercial electrodes. Upon continual cycling from 3 to 6 hours, a second pressure plateau is reached, however, the relative increase in pressure is small (0.46 atm more for the commercial electrodes and 0.12 atm for the Astropower Laboratory electrodes).

The pressure shown in Figure 38 is total pressure and includes the pressure developed, and the vapor pressure of 45 percent KOH. As the vapor pressure of the KOH solution depends only upon temperature, and is the same value in both cases, the plot provides a valid comparison of the gassing of commercial and Astropower Laboratory electrodes. It shows a much smaller degree of gassing for the test electrodes than for the commercial electrodes at 100°C as well as at room temperature.

3.2.5 Performance Demonstration Tests

During the third quarter of Contract NAS 3-6007 a standard test cell design based on the experimental efforts carried out throughout the previous quarters was established. The electrode formulations were selected based upon extended cycle performance previously demonstrated. Astroset Type 5-036-011 inorganic separators were also standardized as to formulation, thickness, transverse strength, porosity, reproducibility, and quality. This standard test cell design was then recommended to the NASA Project Officer for incorporation into the demonstration cells required by the contract and was approved for this purpose.

The test cell design used in the demonstration cells represents a modification of the original test cell which consisted of electrode compartments, gaskets and spacers machined from Teflon and assembled by bolting the components together. The bolted cell design offered many advantages, such as ease of disassembly for inspection of electrodes and separators. In the design used for the demonstration cells, only two case components were required which were assembled along with the separator and electrodes by cementing with an epoxy. The improved cell design was smaller, more compact, and has only one joint making it possible to produce test cells which are leak tight at both room temperature and 100°C during cycle testing.

The test cell cases were machined from inorganically filled Teflon which is highly resistant to concentrated KOH at both ambient and temperatures as high as 150°C. The two halves of the test cell were cemented together after assembly of the battery components, using Epibond 123, supplied by Furane Plastics, Inc., Burbank, California.

The contract work statement specified that eight (8) standard demonstration cells having 0.5 to 0.6 ampere-hour capacity were to be fabricated, formed in accordance with the standard procedures and subjected to life cycle tests as follows:

(1) 2 test cells cycled at 100°C on a 1/2 hour discharge and one-hour charge schedule at 25% depth of discharge (250 ma based on 0.5 ampere-hour cell capacity).

(2) 2 test cells cycled at 100°C on a 1/2 hour discharge and one-hour charge schedule at 50% depth of discharge (500 ma).

(3) 2 test cells cycled at 50°C on a 1/2 hour discharge and one-hour charge schedule at a 25% depth of discharge.

(4) 2 test cells cycled at 25°C on a 1/2 hour discharge and one-hour charge schedule at a 25% depth of discharge (250 ma).

Table XV lists the demonstration test cells and shows the charge-discharge rates and the number of cycles completed. The data presented in this table shows that contract requirements relating to extended cycle life of the silver-zinc demonstration cells at 25% and 50% depth of discharge have been accomplished at 100°, 50°, and 25°C.

Two test cells, (Nos. 3242-01 and 3242-30) were cycle tested at 100°C at 25% depth of discharge on a 1/2 hour discharge-one-hour charge test schedule. The cells received a 10% overcharge on each cycle.

Test Cell No. 3242-01 successfully completed 575 cycles. After 544 cycles the positive electrode current collector tab was broken during a routine cell voltage check. An extension tab was soldered to the remaining tab and the cell was cycled until the test was discontinued based upon reduced

TABLE XV

PERFORMANCE DEMONSTRATION CYCLE TESTS

Test Cell Number	Cycle Test Temperature	Discharge		Charge		Depth of Discharge Percent	Cycles Completed
		Time (hr)	Current (ma)	Time (hr)	Current (ma)		
3242-01	100°C	0.5	250	1.0	138	25	575
3242-30	100°C	0.5	250	1.0	138	25	752
3253-01	100°C	0.5	500	1.0	325	50	483
3253-30	100°C	0.5	500	1.0	325	50	550
3266-01	50°C	0.5	250	1.0	150	25	390*
3240-30	50°C	0.5	250	1.0	138	25	260
3241-01	25°C	0.5	250	1.0	150	25	594*
3241-30	25°C	0.5	250	1.0	150	25	838*

*Tests still running.

charge acceptance. Analysis of the cell following disassembly showed that the zinc electrode was about 30% depleted. The silver electrode was in satisfactory condition except for the broken tab. The inorganic separator showed some surface erosion in the area of the broken current collector tab. This erosion was caused by high current density localized in the area of the tab break.

Test Cell No. 3242-30 was tested following the same schedule used for Cell No. 3242-01. Seven hundred and fifty-two cycles were obtained at 100°C at 25% depth of discharge. The test was discontinued in this particular test due to loss of capacity resulting from zinc electrode changes.

The next series of cycle tests included Test Cell Nos. 3253-01 and 3253-30 which were tested at 50% depth of discharge at 100°C on a 1/2 hour discharge-one hour charge schedule. These cells were given a 30% overcharge. The results of these tests, (Table XV), indicate capability for long cycle life at 50% depth of discharge at 100°C. Test Cell No. 3253-01 completed 483 cycles. The test was discontinued due to depletion of the zinc electrode. Test Cell No. 3253-30 completed 550 cycles on the same test schedule. Disassembly of the cell showed that both electrodes and the inorganic separator were in excellent condition. The zinc electrode had turned blue as a result of this test.

Test Cell Nos. 3266-01 and 3240-30 were cycle tested at 50°C on a 1/2 hour discharge and one-hour charge schedule. These cells were discharged at 25% depth of discharge. Test Cell No. 3240-30 completed 260 cycles when cycle test equipment malfunction occurred during unscheduled working hours and reversed the test cell for an unknown period of time. After the equipment was repaired the cell would not regain full capacity and was disassembled. Examination of the components showed that the silver electrode was in excellent condition. The zinc electrode, however, had slumped in the electrode cavity to a slight extent and was hard and dry. The inorganic separator appeared to be in good condition.

Test Cell No. 3266-01 was also tested at 50°C in accordance with the same test schedule as Test Cell No. 3240-30. At the end of the contract period this cell had completed 390 cycles and was continuing under cycle test.

The last group of demonstration test cells (Nos. 3241-01 and 3241-30) were tested at room temperature at 25% depth of discharge on a 1/2 hour discharge and one-hour charge cycle. A 10% overcharge was used. Test Cell No. 3241-01 completed 594 cycles at the conclusion of the contract, and continues under test.

Test Cell No. 3241-30 completed 838 cycles and is still under test.

4.0 CONCLUSIONS

The experimental work done under Contract NAS 3-6007 resulted in the development of silver-zinc test cells using Astroset Type 5-036-011 inorganic separators and novel electrode configurations which met or exceeded all work statement requirements and goals. It has been demonstrated that:

1. Silver-zinc test cells of this type are capable of long cycle life at both 100° and 25°C. Test cells have completed as many as 2286 cycles at 100°C and 2704 cycles at 25°C on a 1/2 hour discharge-1 hour charge test schedule at a depth of about 17%. Several other test cells exceeded 1500 cycles at both temperatures.
2. The test cells developed in this program also demonstrated capability for operation at 150° and 125°C.
3. Experimental silver-zinc cells built with commercial electrodes and an Astroset Type 5-036-011 inorganic separator ran for more than 200 cycles. Voltage performance was comparable to commercial cells at the same current density at 25°. Cycle test failures of these cells using commercial electrodes were related to electrode changes, not the separators.
4. The gassing characteristics of Astropower Laboratory silver-zinc electrodes were determined to be superior to electrodes removed from a commercial cell and tested with an Astroset Type 5-036-011 inorganic separator at both 25° and 100°C.
5. Astroset Type 5-036-011 inorganic separators are capable of more than 2200 cycles at 100°C and 25°C at practical drain rates. They are also capable of operation at 125° and 150°C.
6. Paste type silver electrodes, as described in this report, are capable of as many as 2280 cycles at 100°C and 25°C and of operation at 125° and 150°C.
7. Paste type zinc electrodes as described in this report are capable of more than 2280 cycles at 100°C and 25°C. They are also

capable of operation at 125^{o} and $150^{o}C$. However, zinc electrode deterioration does occur after prolonged cycling and at high temperature. As the results herein reported indicate that the present zinc electrode system is a limiting factor as to cycle life, improvements in zinc electrode performance should be made in order to take full advantage of the overall capabilities of this design approach.

REFERENCES

1. Frances, H. T., "Space Batteries." Armour Research Foundation NASA SP-5004 (1964).

2. Schutt, R. W. and W. T. Stafford, "The State of Development of Silver-Zinc and Nickel Cadmium Batteries," Space Technology Laboratories (1960.

3. Cooper, J. E., "Characteristics of Separator for Alkaline Silver-Oxide Secondary Batteries," Wright-Patterson Air Force Base (1964).

4. Douglas Proprietary Program 81365-001.

5. Douglas Proprietary Program 81365-002.

6. Douglas Proprietary Program 81365-004.

7. Personal Communication, Dr. J. Lander.

8. Astropower Laboratory Proposal SM-48461-P (1965).

9. "Dial-A-Volt," General Resistance, Inc., New York 55, New York.

10. Jakobi, W., "Alkaline Secondary Cells," Encyclopedia of Chemical Technology, Vol. 3, Second Edition, J. Wiley and Sons (1963).

11. Chapman, C. L., "Technical Problems Associated with the Silver-Zinc Battery, "International Symposium on Batteries, October 21-23, 1958.

12. Hampton, N. A., M. J. Tarbox and J. T. Lilley, Electrochemical Technology, 2, 305 (1964).

13. Young, L., "Anodic Oxide Films, "Academic Press, p.313 (1961).

14. Huber, K., Zeit.Fur. Electrochem., 48, 26 (1942).

15. Collins, D. H., Batteries, The MacMillan Company, p.197 (1963).

16. Christie, G. L., "A Review of Zinc as an Anode Material, Technical Note No. 64-6, Defense Chemical Biological and Radiation Laboratories, Ottawa, Canada, June 1964, (A.D. No. 444536).

17. Hampton, N. A., and M.J. Tarbox, Journal of Electrochemical Soc., 110, 95, (1963).

APPENDIX A

VIBRATION TEST

The test cell will be securely mounted in a text fixture specifically designed to support the cell in any of the three mutually perpendicular axes for vibration tests. A 6-100 shaker system will be used to perform these tests. The test cell will remain electrically inoperative throughout the vibration tests.

A resonant survey test will be performed to determine the resonant modes of the test fixture and cell. A frequency sweep will be made from five to 16 cps with a displacement amplitude of 0.368 inch and from 16 to 2000 cps at 5 G peak. This frequency sweep shall be performed once along each of the three mutually perpendicular axes. The accelerometer pickup will be placed at the mounting interface between the vibration fixture and the test cell. During each frequency sweep in each direction, all resonant frequency points will be recorded. The duration of each frequency sweep in each axis will be one minute from five to 16 cps and ten minutes from 16 to 2000 cps. A resonant frequency test at one-half of each resonant frequency resulting from the resonant frequency sweep noted above, will be performed for a period of 30 minutes for each resonant frequency.

At the conclusion of each vibration test in each of the three mutually perpendicular axes, the cell will be examined for cracks, dents or other damage. If there are no evidences of damage, the cell is acceptable for performing the next vibration test.

APPENDIX B

QUALITY ASSURANCE PROVISIONS

The quality assurance aspects of (1) the incoming materials used to fabricate the test cells, (2) the fabrication processes and assembly techniques of the test cells, (3) the testing procedures, and (4) the instrumentation calibration methods, have been emphasized throughout the testing phase of the program.

Detailed material specifications were established to which all incoming raw materials were inspected and certified prior to incorporation into test cells. Also, detailed process specifications were written covering the entire fabrication and assembly of all parts of the test cells. As improved fabrication and assembly techniques were incorporated, the corresponding process specifications were immediately revised to reflect the approved changes.

Cell testing and instructions were provided in written form to the laboratory technicians. Recorder instrument charts were identified and filed in individual test cell folders, along with all other test cell data.

A program of test equipment calibration and evaluation as specified in the contract was established. All data acquisition equipment was calibrated at regular intervals and at other times as deemed necessary in order to insure an adequate level of accuracy at all times. A record of this calibration information was maintained in a Research Notebook and this information was available for inspection. Douglas/Astropower Laboratory's primary standard used for instrument calibration was a Weston Model 4 Standard Cell which possessed a high level of accuracy which was traceable to the National Bureau of Standards. A Leeds and Northrup Model 8687 Volt Potentiometer was used as a secondary standard for calibration and its accuracy was evaluated prior to use by comparison with the primary standard. A Dynamics Instrumentation Corporation Model 4072 Volt-Milliammeter calibrated for accuracy against the secondary standard was used as a working standard and for making voltage and current measurements where a high degree of accuracy was desired. This instrument was capable of reading voltage directly to 0.1 volt, and 0.01 volt could be approximated with an accuracy of ± 0.01 volts. A second Dynamics instrument was employed so that one instrument was used exclusively as a working standard and the second instrument was used for making precision voltage and current measurements.

The contract specified that the equipment used for the purpose of obtaining data was to be calibrated, evaluated, controlled, and maintained to ensure reliability and accuracy. The calibration was to be at scheduled intervals or prior to and after usage. Douglas Aircraft Company's Standard Practice Bulletin No. 714 outlines the policies and responsibilities related to the accomplishment of maintenance, repair and certification of test equipment and to the maintenance of records of such action. All of the data acquisition equipment used in the program was subjected to scheduled certification by Douglas Aircraft Company. Such equipment included recording instruments, voltmeters, milliammeters, power supplies, vacuum tube volt-milliammeters, and decade resistance boxes. The scheduled certification periodically designates that the test equipment has been property calibrated, checked and meets the requirements of the certification instructions. This certification is evidenced by a "Certified" Douglas Aircraft Company label affixed to the piece of test equipment and validated in accordance with Standard Practice Bulletin No. 714.